

**Fig. 4.** Effects of *Chlorella* on activation of astrocytes. Activated astrocytes in the hippocampal CA1 region were immunostained using anti-GFAP antibody and anti-Iba1 antibody after 16-month *Chlorella* consumption. Representative pictures are shown (A, B and C). Arrows indicate activated astrocytes. Scale bar: 100  $\mu$ m. (A) DAL101 (normal diet), (B) DAL101 (*Chlorella* diet), and (C) wild type (C57BL/6 with normal diet). (D) Positive cells in a single visual field in the hippocampal CA1 region were counted in a blinded fashion. (E) and (F) show anti-Iba1-positive cells in hippocampus and the CA1 region, respectively. DAL101: DAL101 normal diet ( $n=8$ ), +*Chlorella*: DAL101 with *Chlorella* diet ( $n=7$ ), and wild type: C57BL/6 with normal diet ( $n=6$ ). \*\* $p < 0.01$ : significant vs. DAL101 (normal diet).

deficiency affects the growth of animals (Supplementary Table 1). Prolonged consumption of *Chlorella* significantly improved the growth of DAL101, and reached the wild-type level (Supplementary Table 1), clearly indicating that *Chlorella* has a benefit to DAL101 growth.

First, the Morris water-maze test was performed to investigate the effects of a prolonged consumption of *Chlorella* on the decline in spatial memory and learning abilities of DAL101 mice. The physical strength of male DAL101 mice markedly decreases with aging, as reported previously [19]; however, female DAL101 can be subjected to the test because swimming speed of female DAL101 mice was not affected until 18 months old as reported previously [19]. A training trial to find a hidden platform was performed for 5 days, and then the time to reach the hidden platform was measured (Fig. 2). After *Chlorella* was fed for 10 months from 8 weeks of age, there was no difference among the DAL101 group without *Chlorella*, the DAL101 group with *Chlorella* and the wild-type group in the time required to reach the platform. As reported [16],

DAL101 is still young at 12 months old (*Chlorella* diet for 10 months from 8 weeks of age) and no symptom of memory loss and cognitive decline appeared. After DAL101 mice had been fed for 16 months, the Morris water-maze test was performed. In this test, DAL101 mice with the *Chlorella* diet reached the hidden platform significantly faster than DAL without *Chlorella* (Fig. 2B), suggesting that prolonged *Chlorella* consumption suppressed the decline in spatial memory and learning. In a probe trial performed the day after completing the 5-day training trial, DAL101 with *Chlorella* showed only a trend of a longer stay in the targeted quadrant (Fig. 2C).

Next, an alternative test was performed to confirm the effects of 16-month long-term *Chlorella* consumption. The object recognition test is not influenced by physical ability and the sniffing frequency was not significantly decreased even in old male DAL101 (data not shown). Thus, this test involved both male and female DAL101 mice. The animals explored 2 different objects for 10 min during the training period. As a result of the training trial, all control, *Chlorella*

treatment, and normal groups approached or sniffed the 2 objects with the same frequency (~50% of recognition index) (Fig. 3A), indicating comparable attention, motivation and visual perception. One day after training, one of the conditioned objects was replaced with a novel object. During 5-min testing, aged DAL101 with normal diet approached or sniffed the novel object at the same frequency as the original object (Fig. 3B). These results indicated that aged DAL101 showed a deficit in visual recognition memory. In contrast, DAL101 with the *Chlorella* diet showed an intact ability to detect the novel object at high frequency and reached the level of the wild type, indicating that this age-dependent deficit in recognition memory was significantly prevented by the *Chlorella* diet.

Increased astrocyte activation is a marker of inflammation and remodeling in brain impairment [2]. To investigate the effects of *Chlorella* on the central nervous system in DAL101, the number of reactive astrocytes in the hippocampal CA1 region was examined by immunohistological staining (Fig. 4A–C). The number of activated astrocytes immunostained with anti-GFAP antibody in the hippocampal CA1 region was significantly greater in DAL101 than in wild-type mice (Fig. 4D). On the other hand, we could not find significant difference in anti-Iba 1 antibody staining, a marker of gliosis [3] (Fig. 4E and F). Since the number of activated astrocytes increases when the brain is injured, the brain of DAL101 mice may have been affected 16 months after experiment initiation, probably by accelerated aging. In contrast, the number of activated astrocytes in DAL101 with the *Chlorella* diet was similar to that in wild-type mice, suggesting that *Chlorella* prevented brain injury in DAL101 mice (Fig. 4D).

We investigated the effects of long-term *Chlorella* consumption on oxidative stress, body weight, age-dependent cognitive ability and the central nervous system, and found benefits of *Chlorella* from all points of view.

AD manifests with impaired memory, and finally leads to severe dementia through progressive memory/cognitive disorder. Since DAL101 exhibited a shortened life span, age-dependent neurodegeneration, hyperphosphorylation of tau and decline in cognitive ability, this model mouse is suitable to explore foods that prevent dementia by long-term feeding [16]. We investigated the effects of 16-month *Chlorella* consumption on spatial learning/memory (Morris water-maze test) and object recognition ability (novel object recognition test) using DAL101 mice and found that long-term *Chlorella* consumption prevented cognitive impairment in DAL101.

Increased activated astrocytes are a marker of inflammation and remodeling [2]. Prolonged *Chlorella* consumption significantly decreased activated astrocytes in the hippocampal CA1 region in aged DAL101, suggesting that *Chlorella* may suppress inflammation, perhaps owing to its antioxidative ability.

DAL101 mice cannot efficiently degrade aldehydes, such as 4-HNE, because their ALDH activity is suppressed [16,17]. An increase in the 4-HNE level in patients with mild cognitive disorder (MCI) and early stage AD, compared to that in healthy subjects, has been reported [32], which is consistent with the findings regarding oxidative stress markers in cerebrospinal fluid [20]. Moreover, elevation of the oxidative stress level has been observed in a mouse AD model with amyloid  $\beta$ -protein (A $\beta$ ) deposits [21]. Based on these findings, oxidative stress seems to play a crucial role before AD onset.

*Chlorella* is rich in chloroplasts, where plastoquinone substitutes for ubiquinone as an electron carrier in the photosynthetic electron transport chain. Plastoquinone shows the better antioxidant properties, as shown in chemical experiments [7] and is not complicated by danger of prooxidant effect within a large range of concentrations [27]. It is possible that plastoquinone acts as better antioxidant to prevent the cognitive decline.

Elevated blood homocysteine has been reported to be a risk factor for cardiovascular disease, cerebral stroke, and AD [25]. It has also been reported that elevated blood homocysteine associated with folic acid deficiency increased the cytotoxicity of A $\beta$  in a mouse AD model, in which A $\beta$  accumulates [8]. Insufficient folic acid and vitamin B6 and B12 intake increases homocysteine [9]. *Chlorella* is rich in folic acid (1000–3000  $\mu$ g/100 g) in addition to antioxidants [22,26]. Thus, it is possible to speculate that *Chlorella* improves cognitive ability in DAL101 mice through the interaction of folic acid and antioxidants. Even if a single dietary antioxidant exhibits no preventive effect, multi-compounds such as *Chlorella* may be efficient to prevent age-dependent disorders.

## Appendix A. Supplementary data

Supplementary data associated with this article can be found, in the online version, at doi:10.1016/j.neulet.2009.08.044.

## References

- [1] T. Hasegawa, Y. Kimura, K. Hiromastu, N. Kobayashi, A. Yamada, M. Makino, M. Okuda, T. Sano, K. Nomoto, Y. Yoshikai, Effect of hot water extract of *Chlorella vulgaris* on cytokine expression patterns in mice with murine acquired immunodeficiency syndrome after infection with *Listeria monocytogenes*, *Immunopharmacology* 35 (1997) 273–282.
- [2] O. Isacson, W. Fischer, K. Victorin, D. Dawbarn, A. Bjorklund, Astroglial response in the excitotoxically lesioned neostriatum and its projection areas in the rat, *Neuroscience* 20 (1987) 1043–1056.
- [3] D. Ito, Y. Imai, K. Ohsawa, K. Nakajima, Y. Fukuuchi, S. Kohsaka, Microglia-specific localisation of a novel calcium binding protein, Iba1, *Brain Res. Mol. Brain Res.* 57 (1998) 1–9.
- [4] S.A. Jo, E.K. Kim, M.H. Park, C. Han, H.Y. Park, Y. Jang, B.J. Song, I. Jo, A Glu487Lys polymorphism in the gene for mitochondrial aldehyde dehydrogenase 2 is associated with myocardial infarction in elderly Korean men, *Clin. Chim. Acta* 382 (2007) 43–47.
- [5] K. Kamino, K. Nagasaka, M. Imagawa, H. Yamamoto, H. Yaneda, A. Ueki, S. Kitamura, K. Namekata, T. Miki, S. Ohta, Deficiency in mitochondrial aldehyde dehydrogenase increases the risk for late-onset Alzheimer's disease in the Japanese population, *Biochem. Biophys. Res. Commun.* 273 (2000) 192–196.
- [6] F. Konishi, K. Tanaka, K. Himeno, K. Taniguti, K. Nomoto, Antitumor effect induced by a hot water extract of *Chlorella vulgaris* (CE): resistance to Meth-A tumor growth mediated by CE-induced polymorphonuclear leukocytes, *Cancer Immunol. Immunother.* 19 (1985) 73–78.
- [7] J. Kruk, M. Jemiola-Rzeminska, K. Strzalka, Plastoquinol and alpha-tocopherol quinol are more active than ubiquinol and alpha-tocopherol in inhibition of lipid peroxidation, *Chem. Phys. Lipids* 87 (1997) 73–80.
- [8] I.I. Kruman, T.S. Kumaravel, A. Lohani, W.A. Pedersen, R.G. Cutler, Y. Kruman, N. Hanghey, J. Lee, M. Evans, M.P. Mattson, Folic acid deficiency and homocysteine impair DNA repair in hippocampal neurons and sensitize them to amyloid toxicity in experimental models of Alzheimer's disease, *J. Neurosci.* 22 (2002) 1752–1762.
- [9] R. Leboeuf, Homocysteine and Alzheimer's disease, *J. Am. Diet Assoc.* 103 (2003) 304–307.
- [10] H.S. Lee, C.Y. Choi, C. Cho, Y. Song, Attenuating effect of chlorella supplementation on oxidative stress and NF $\kappa$ B activation in peritoneal macrophages and liver of C57BL/6 mice fed on an atherogenic diet, *Biosci. Biotechnol. Biochem.* 67 (2003) 2083–2090.
- [11] M.A. Lovell, W.D. Ehmann, M.P. Mattson, W.R. Markesbery, Elevated 4-hydroxynonenal in ventricular fluid in Alzheimer's disease, *Neurobiol. Aging* 18 (1997) 457–461.
- [12] A. Maczurek, K. Hager, M. Kenkies, M. Sharman, R. Martins, J. Engel, D.A. Carlson, G. Munich, Lipoic acid as an anti-inflammatory and neuroprotective treatment for Alzheimer's disease, *Adv. Drug Deliv. Rev.* 60 (2008) 1463–1470.
- [13] M.P. Mattson, Pathways towards and away from Alzheimer's disease, *Nature* 430 (2004) 631–639.
- [14] R.G. Morris, P. Garrud, J.N. Rawlins, J. O'Keefe, Place navigation impaired rats with hippocampal lesions, *Nature* 297 (1982) 681–683.
- [15] I. Ohsawa, K. Nishimaki, C. Yasuda, K. Kamino, S. Ohta, Deficiency in a mitochondrial aldehyde dehydrogenase increases vulnerability to oxidative stress in PC12 cells, *J. Neurochem.* 84 (2003) 1110–1117.
- [16] I. Ohsawa, K. Nishimaki, Y. Murakami, Y. Suzuki, M. Ishikawa, S. Ohta, Age-dependent neurodegeneration accompanying memory loss in transgenic mice defective in mitochondrial ALDH2 activity, *J. Neurosci.* 28 (2008) 6239–6249.
- [17] S. Ohta, I. Ohsawa, Dysfunction of mitochondria and oxidative stress in the pathogenesis of Alzheimer's disease: on defects in the cytochrome c oxidase complex and aldehyde detoxification, *J. Alzheimer's Dis.* 9 (2006) 155–166.
- [18] S. Ohta, I. Ohsawa, K. Kamino, F. Ando, H. Shimokata, Mitochondrial ALDH2 deficiency as an oxidative stress, *Ann. N. Y. Acad. Sci.* 1011 (2004) 36–44.

- [19] D. Pratico, Evidence of oxidative stress in Alzheimer's disease brain and antioxidant therapy: lights and shadows, *Ann. N. Y. Acad. Sci.* 1147 (2008) 70–78.
- [20] D. Pratico, C.M. Clark, F. Liun, J. Rokach, V.Y. Lee, J.Q. Trojanowski, Increase of brain oxidative stress in mild cognitive impairment: a possible predictor of Alzheimer disease, *Arch. Neurol.* 59 (2002) 972–976.
- [21] D. Pratico, K. Uryu, S. Leight, J.Q. Trojanowski, V.M. Lee, Increased lipid peroxidation precedes amyloid plaque formation in an animal model of Alzheimer amyloidosis, *J. Neurosci.* 21 (2001) 4183–4187.
- [22] R. Pratt, E. Johnson, Production of thiamine, riboflavin, folic acid, and biotin by *Chlorella vulgaris* and *Chlorella pyrenoidosa*, *J. Pharm. Sci.* 54 (1965) 871–874.
- [23] M. Sano, H. Grossman, K. Van Dyk, Preventing Alzheimer's disease: separating fact from fiction, *CNS Drugs* 22 (2008) 887–902.
- [24] C. Schneider, K.A. Tallman, N.A. Porter, A.R. Brash, Two distinct pathways of formation of 4-hydroxynonenal, Mechanisms of nonenzymatic transformation of the 9- and 13-hydroperoxides of linoleic acid to 4-hydroxyalkenals, *J. Biol. Chem.* 276 (2001) 20831–20838.
- [25] S. Seshadri, A. Beiser, J. Selhub, P.F. Jacques, I.H. Rosenberg, R.B. D'Agostino, P.W. Wilson, P.A. Wolf, Plasma homocysteine as a risk factor for dementia and Alzheimer's disease, *N. Engl. J. Med.* 346 (2002) 476–483.
- [26] S. Shibata, Y. Natori, T. Nishihara, K. Tomisaka, K. Matsumoto, H. Sansawa, V.C. Nguyen, Antioxidant and anti-cataract effects of chlorella on rats with streptozotocin induced diabetes, *J. Nutr. Sci. Vitaminol. (Tokyo)* 49 (2003) 334–339.
- [27] V.P. Skulachev, V.N. Anisimov, Y.N. Antonenko, L.E. Bakeeva, B.V. Chernyak, V.P. Elichev, O.F. Filenko, N.I. Kalinina, V.I. Kapelko, N.G. Kolosova, B.P. Kopnin, G.A. Korshunova, M.R. Lichinitser, L.A. Obukhova, E.G. Pasyukova, O.I. Pisarenko, V.A. Roginsky, E.K. Ruuge, I.I. Senin, I.I. Severina, M.V. Skulachev, I.M. Spivak, V.N. Tashlitsky, V.A. Tkachuk, M.Y. Vyssokikh, L.S. Yaguzhinsky, D.B. Zorov, An attempt to prevent senescence: a mitochondrial approach, *Biochim. Biophys. Acta* 1787 (2009) 437–461.
- [28] K. Tanaka, T. Koga, F. Konishi, M. Nakamura, M. Mitsuyama, K. Himeno, K. Nomoto, Augmentation of host defense by a unicellular green alga, *Chlorella vulgaris*, to *Escherichia coli* infection, *Infect. Immun.* 53 (1986) 267–271.
- [29] K. Uchida, 4-Hydroxy-2-nonenal: a product and mediator of oxidative stress, *Prog. Lipid Res.* 42 (2003) 318–343.
- [30] B. Wang, J. Wang, S. Zhou, S. Tan, X. He, Z. Yang, Y.C. Xie, S. Li, C. Zheng, X. Ma, The association of mitochondrial aldehyde dehydrogenase gene (ALDH2) polymorphism with susceptibility to late-onset Alzheimer's disease in Chinese, *J. Neurol. Sci.* 268 (2008) 172–175.
- [31] H. Wang, G.D. Ferguson, V.V. Pineda, P.E. Cundiff, D.R. Storm, Overexpression of type-1 adenylyl cyclase in mouse forebrain enhances recognition memory and LTP, *Nat. Neurosci.* 7 (2004) 635–642.
- [32] T.I. Williams, B.C. Lynn, W.R. Markesbery, M.A. Lovell, Increased levels of 4-hydroxynonenal and acrolein, neurotoxic markers of lipid peroxidation, in the brain in mild cognitive impairment and early Alzheimer's disease, *Neurobiol. Aging* 27 (2006) 1094–1099.
- [33] A. Yoritaka, N. Hattori, K. Uchida, M. Tanaka, E.R. Stadtman, Y. Mizuno, Immunohistochemical detection of 4-hydroxynonenal protein adducts in Parkinson disease, *Proc. Natl. Acad. Sci. U.S.A.* 93 (1996) 2696–2701.

# Protection of the Retina by Rapid Diffusion of Hydrogen: Administration of Hydrogen-Loaded Eye Drops in Retinal Ischemia–Reperfusion Injury

Hideaki Oharazawa,<sup>1</sup> Tsutomu Igarashi,<sup>2</sup> Takashi Yokota,<sup>3</sup> Hiroaki Fujii,<sup>1</sup> Hisabaru Suzuki,<sup>2</sup> Mitsuru Machide,<sup>4</sup> Hiroshi Takabashi,<sup>2</sup> Shigeo Ohta,<sup>5</sup> and Ikuroh Ohsawa<sup>4</sup>

**PURPOSE.** Retinal ischemia-reperfusion (I/R) injury by transient elevation of intraocular pressure (IOP) is known to induce neuronal damage through the generation of reactive oxygen species. Study results have indicated that molecular hydrogen (H<sub>2</sub>) is an efficient antioxidant gas that selectively reduces the hydroxyl radical (·OH) and suppresses oxidative stress-induced injury in several organs. This study was conducted to explore the neuroprotective effect of H<sub>2</sub>-loaded eye drops on retinal I/R injury.

**METHODS.** Retinal ischemia was induced in rats by raising IOP for 60 minutes. H<sub>2</sub>-loaded eye drops were prepared by dissolving H<sub>2</sub> gas into a saline to saturated level and administered to the ocular surface continuously during the ischemia and/or reperfusion periods. One day after I/R injury, apoptotic cells in the retina were quantified, and oxidative stress was evaluated by markers such as 4-hydroxynonenal and 8-hydroxy-2-deoxyguanosine. Seven days after I/R injury, retinal damage was quantified by measuring the thickness of the retina.

**RESULTS.** When H<sub>2</sub>-loaded eye drops were continuously administered, H<sub>2</sub> concentration in the vitreous body immediately increased and I/R-induced ·OH level decreased. The drops reduced the number of retinal apoptotic and oxidative stress marker-positive cells and prevented retinal thinning with an accompanying activation of Müller glia, astrocytes, and microglia. The drops improved the recovery of retinal thickness by >70%.

**CONCLUSIONS.** H<sub>2</sub> has no known toxic effects on the human body. Thus, the results suggest that H<sub>2</sub>-loaded eye drops are a highly useful neuroprotective and antioxidative therapeutic

treatment for acute retinal I/R injury. (*Invest Ophthalmol Vis Sci.* 2010;51:487–492) DOI:10.1167/iovs.09-4089

Retinal ischemia-reperfusion (I/R) injury by transient elevation of intraocular pressure (IOP) in animal models is known to induce necrosis and apoptosis of cells and significant reductions in thickness in multiple layers of the retina.<sup>1,2</sup> Clinically, these features closely resemble several diseases such as acute angle-closure glaucoma, retinal artery occlusion, and amaurosis fugax.<sup>3</sup> It can irreversibly damage the retina, causing visual impairment and blindness. Immediate mechanisms of I/R injury involve the formation of reactive oxygen species (ROS),<sup>4</sup> which has been considered to contribute to the pathogenesis of many neurodegenerative diseases, including glaucomatous neurodegeneration.<sup>5</sup> Endogenous antioxidant enzymes and organic free radical scavengers can retard or prevent neuronal damages of retinal I/R injury in many animal models.<sup>6–13</sup> One highly reactive ROS, hydroxyl radical (·OH), is generated during the early phase of reperfusion after ischemia and a major cause of retinal injury.<sup>14–16</sup> ·OH attacks lipids, proteins and nucleic acids causing irreversible cellular damage.

In the past two decades, much attention has been focused on the use of several pharmaceutical gaseous molecules to attenuate oxidative stress.<sup>17</sup> A variety of gas delivery systems are used and under development for safe and effective administration of medical gases. We have reported that H<sub>2</sub> selectively reduces ·OH and peroxynitrite without affecting other oxygen-derived free radicals.<sup>18</sup> Inhalation of H<sub>2</sub> gas has been demonstrated to limit the infarct volume of the brain, heart, and liver by reducing I/R injury<sup>19–21</sup> and can ameliorate intestinal transplant injury.<sup>22</sup> Moreover, the consumption of water with dissolved H<sub>2</sub> to a saturated level prevents stress-induced cognitive decline and 6-hydroxydopamine-induced nigrostriatal degeneration.<sup>23,24</sup> One clinical trial demonstrated a decrease in low-density lipoprotein after drinking H<sub>2</sub>-loaded water.<sup>25</sup> H<sub>2</sub> has the potential to easily diffuse into organs and no known toxic effects on the human body.<sup>18</sup>

We have therefore developed a simple and effective method to deliver H<sub>2</sub> into lesions. The method is H<sub>2</sub>-loaded eye drops, which are convenient, compared with the inhalation of H<sub>2</sub> gas, for the treatment of eye diseases. In this article, we demonstrate that the continuous administration of H<sub>2</sub>-loaded eye drops immediately increases H<sub>2</sub> concentration in the vitreous body and prevents I/R-induced oxidative stress, leading to a decrease in apoptotic cell death in the retina and a decrease in retinal thinning with glial responses.

From the <sup>1</sup>Department of Ophthalmology, Musashikosugi Hospital, Nippon Medical School, Kanagawa, Japan; the <sup>2</sup>Department of Ophthalmology, Nippon Medical School, Tokyo, Japan; and the <sup>3</sup>Department of Molecular Biology, <sup>4</sup>The Center of Molecular Hydrogen Medicine, and the <sup>5</sup>Department of Biochemistry and Cell Biology, Institute of Development and Aging Sciences, Nippon Medical School, Kanagawa, Japan.

Supported in part by Ministry of Education, Culture, Sports, Science, and Technology of Japan Grants-in-Aid 19659331 (SO) and 20500345 (IO).

Submitted for publication June 4, 2009; revised July 28 and accepted August 11, 2009.

Disclosure: H. Oharazawa, None; T. Igarashi, None; T. Yokota, None; H. Fujii, None; H. Suzuki, None; M. Machide, None; H. Takahashi, None; S. Ohta, None; I. Ohsawa, None

Corresponding author: Ikuroh Ohsawa, The Center of Molecular Hydrogen Medicine, Institute of Development and Aging Sciences, Nippon Medical School, 1-396 Kosugi-cho, Nakahara-ku, Kawasaki, 211-8533 Japan; iohsawa@nms.ac.jp.

## METHODS

### Administration of H<sub>2</sub> and Measurement of Its Concentration

H<sub>2</sub>-loaded eye drops were prepared by bubbling H<sub>2</sub> gas (flow rate: 1 L/min) through 400 mL of normal saline solution with stirring for 10 minutes to a saturated level (Fig. 1A), and then stored in an aluminum foil bag (Fig. 1B; Hosokawa Yoko, Tokyo, Japan) with no dead volume. The concentration of H<sub>2</sub> in the bag slowly decreased with a half-life of approximately 3 months. Freshly prepared H<sub>2</sub>-loaded eye drops were administered to the ocular surface continuously (4 mL/min) with a dropper connected to the aluminum foil bag during the ischemia and/or reperfusion periods. The H<sub>2</sub> dissolved in saline solution was measured by using a needle-type H<sub>2</sub> sensor (Unisense, Aarhus N, Denmark). The H<sub>2</sub> concentration on the ocular surface was measured by touching the sensor to the surface. H<sub>2</sub> concentration was measured in the vitreous body by inserting the sensor into the vitreous body through the sclera.

To investigate the effect of H<sub>2</sub>-loaded eye drops on retinal I/R injury, we applied them using four different time courses (see Fig. 4A): duration F, eye drops with and without H<sub>2</sub> were applied during an

entire 90-minute process (60 minutes of ischemia followed by 30 minutes of reperfusion); duration I, eye drops with H<sub>2</sub> were applied only during ischemia; duration R, eye drops with H<sub>2</sub> were applied only after reperfusion; and duration I/R, eye drops with H<sub>2</sub> were applied for 10 minutes before and 30 minutes after reperfusion.

### Induction of I/R Injury

Retinal I/R injury was induced essentially as described previously.<sup>2,26</sup> Seven-week-old male Sprague-Dawley rats weighing 200 to 250 g were anesthetized with an intraperitoneal injection of pentobarbital (100 mg/kg), and the pupils were dilated with topical phenylephrine hydrochloride and tropicamide. After topical application of 0.4% oxybutyrocaine hydrochloride, the anterior chamber was cannulated with a 30-gauge infusion needle connected to a normal saline reservoir. The IOP was raised to 110 mm Hg for 60 minutes by elevating the saline reservoir. Body temperature was maintained at 37.0 ± 0.5°C with a rectal thermometer probe and a heating pad during the experimental period. Retinal ischemia was confirmed by whitening of the iris and fundus. After 60 minutes of ischemia, the needle was withdrawn from the anterior chamber and the intraocular pressure was normalized. The animals were euthanized with an overdose of anesthesia after reperfusion, and the eyes were immediately enucleated. All animals were treated in accordance with the ARVO Statement for the Use of Animals in Ophthalmic and Vision Research. The studies were approved by the Animal Care and Use Committee of Nippon Medical School. All experiments were performed by examiners blinded to the genotypes or treatments of the rat.

### Detection of ·OH

The procedure for the measurement of accumulated ·OH in the eye is similar to that previously described with modifications.<sup>27</sup> We used 2-[6-(4'-hydroxyphenoxy)-3H-xanthen-3-on-9-yl] benzoate (HPF; Daiichi Pure Chemicals, Tokyo, Japan), which detects highly reactive ROS including ·OH, as a fluorescence probe.<sup>28</sup> HPF (4 μL, 1 mM) was given intravitreally just before the induction of ischemia. Rats were killed after 60 minutes of ischemia followed by 15 minutes of reperfusion. Retinas were quickly removed and flat mounted without fixation. The fluorescence images were acquired by using a laser scanning confocal microscope. The acquired images were analyzed by quantitative comparisons of the relative fluorescence intensity of retinas between groups (NIH Image software, developed by Wayne Rasband, National Institutes of Health, Bethesda, MD; available at <http://rsb.info.nih.gov/ij/index.html>).

### Histopathologic and Morphometric Study

Eyes were enucleated 7 days after reperfusion and fixed in 1% glutaraldehyde and 4% paraformaldehyde (PFA) in 0.1 M phosphate-buffered saline (PBS) for 30 minutes, and the anterior segments were removed. Corneas and lenses were discarded. The entire eye cups were further fixed in the same solution overnight and then transferred to 30% sucrose for cryoprotection. Cryosections (10 μm thick) were cut along the vertical meridian of the eye, passing through the optic nerve head, and were stained with hematoxylin and eosin (H&E). Retinal damage was assessed by measuring the thickness of the retina.<sup>1</sup> The thickness is defined as the total width between the inner limiting membrane to the interface of the outer plexiform layer and the outer nuclear layer. These measurements were made at a distance within 1 to 2 mm from the optic disc using a light microscope. The value was averaged from four measurements in the temporal and nasal hemispheres of three different sections.

### TUNEL Assay and Immunohistochemical Staining

One day or 7 days after reperfusion, the eyes were immediately enucleated. For TUNEL assay and the staining of reactive gliosis markers, they were fixed in 4% PFA, and for staining of oxidative stress markers they were fixed in Bouin's fluid for 30 minutes. Next, the anterior

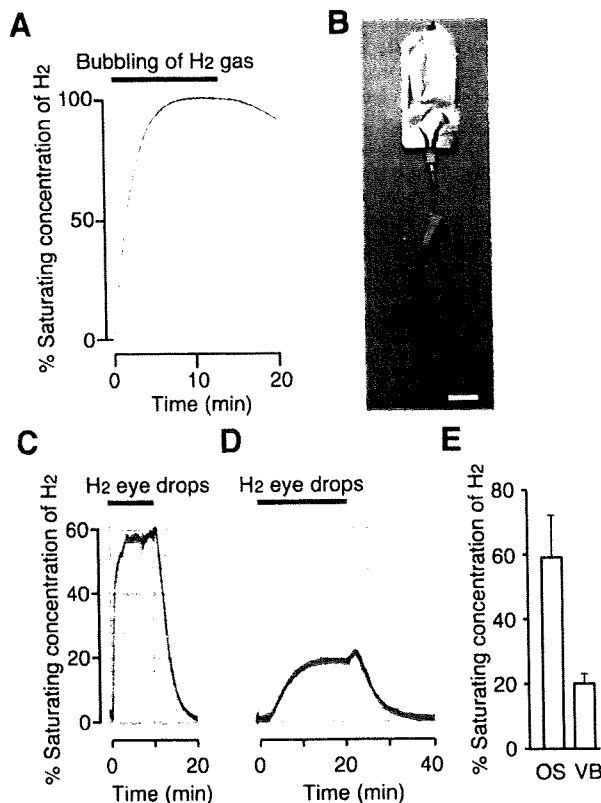


**FIGURE 1.** H<sub>2</sub>-loaded eye drops increased intravitreal H<sub>2</sub>. (A) H<sub>2</sub>-loaded eye drops were prepared by bubbling H<sub>2</sub> gas (solid thick line, flow rate: 1 L/min) through 400 mL of normal saline solution. After the bubbling was stopped, the H<sub>2</sub> concentration was gradually decreased by stirring and reached <1% within 90 minutes. (B) H<sub>2</sub>-loaded eye drops were stored in an aluminum foil bag and administered to the ocular surface with a dropper. Scale bar, 4 cm. The concentrations of H<sub>2</sub> on the ocular surface (C) and in the vitreous body (D) were monitored with a needle-type H<sub>2</sub> sensor. Solid thick line: application times of H<sub>2</sub>-loaded eye drops (4 mL/min). (E) Summary data showing H<sub>2</sub> concentration on the ocular surface (OS; n = 3) and in the vitreous body (VB; n = 3). Data represent the mean ± SD.

segments were removed and the corneas and lenses were discarded. For the TUNEL assay and for the staining of reactive gliosis markers, the obtained entire eye cups were further fixed in the same solution overnight. For the staining of oxidative stress markers, they were further fixed in the same solution for 2 hours. After cryoprotection with 30% sucrose, cryosections (10  $\mu$ m thick) were cut along the vertical meridian of the eye, passing through the optic nerve head. TUNEL staining was performed with an apoptosis detection kit according to the supplier's instructions (Chenicon, Norcross, GA).<sup>29</sup> The numbers of TUNEL-positive cells in the retina were counted at a final magnification  $\times 200$  for each section using a light microscope.

For the immunostaining of oxidative stress markers, 4-hydroxynonenal (4-HNE) and 8-hydroxy-2-deoxyguanosine (8-OHdG),<sup>30,31</sup> cryosections were postfixed in acetone and stained using the ABC kit according to the supplier's instructions (Vector Laboratories, Burlingame, CA).<sup>18</sup> Sections were incubated with the following primary antibodies: mouse monoclonal anti-4-HNE (1:400; JaICA, Shizuoka, Japan) and mouse monoclonal anti-8-OHdG (1:20; JaICA), in a blocking buffer for 1 hour at 4°C. The stained sections were further counterstained for nuclei with methyl green (0.5%). A light microscope was used to count the number of 4-HNE- and 8-OHdG-positive cells in each section of the retina at a final magnification of  $\times 200$ .

For immunofluorescent staining of microglia and macroglia (astrocytes and Müller cells), cryosections were incubated with the following primary antibodies: rabbit polyclonal anti-Iba1<sup>32</sup> (1:100; Wako, Osaka, Japan) or rabbit polyclonal anti-gliial fibrillary acidic proteins (GFAP; 1:500; DAKO, Glostrup, Denmark) in blocking buffer for 1 hour at room temperature. After they were washed twice with PBS, the sections were incubated with fluorescein isothiocyanate (FITC)-conjugated secondary antibody (1:100; Invitrogen, Carlsbad, CA) for 30 minutes and further counterstained for nuclei with propidium iodide for 10 minutes. A laser scanning confocal microscope (FV300; Olympus, Tokyo, Japan) was used to count the number of Iba1-positive cells in each section of the retina at a final magnification of  $\times 200$ .

### Statistical Analysis

All data are presented as the mean  $\pm$  SD. For single comparisons, we performed an unpaired two-tailed Student's *t*-test. For multiple comparisons, we used an analysis of variance (ANOVA) followed by the Fisher least-significant difference (LSD) test (StatView; SAS Institute, Cary, NC). *P* < 0.05 was considered statistically significant.

## RESULTS

### Effect of H<sub>2</sub>-Loaded Eye Drops on H<sub>2</sub> Concentration in the Vitreous Body and the Accumulation of $\cdot$ OH during Retinal I/R

We prepared an H<sub>2</sub>-saturated normal saline solution (0.8 mM, pH 7.2; H<sub>2</sub>-loaded eye drops) and packed it into an aluminum foil bag to prevent a decrease in H<sub>2</sub> concentration. A dropper connected to the bag was held close to the rat's eye, and drops were applied to the ocular surface. The time-course of changes in H<sub>2</sub> levels was monitored with a needle-shaped hydrogen sensor electrode inserted through the sclera to the vitreous body. When H<sub>2</sub>-loaded eye drops were administered continuously, approximately 0.5 mM H<sub>2</sub> was detected on the ocular surface (Fig. 1C). Two minutes after the start of administration, H<sub>2</sub> concentration in the vitreous body started to increase and reached a maximum level after 15 minutes (Fig. 1D). At that time, the H<sub>2</sub> concentration accounted for approximately 20% (0.16 mM) of the H<sub>2</sub>-loaded eye drops. Immediately after administration of the H<sub>2</sub>-loaded eye drops ceased, the H<sub>2</sub> concentration in the vitreous body was observed to gradually decrease and then completely disappear after 15 minutes (Fig. 1D). The maximum observed concentration of H<sub>2</sub> in the vitreous body

was approximately one third of that observed on the ocular surface (Fig. 1E).

To verify that the diffused H<sub>2</sub> protects against  $\cdot$ OH during retinal I/R, we assessed the accumulation of  $\cdot$ OH by the fluorescence signal emitted by the oxidized form of HPF.<sup>28</sup> We produced retinal ischemia in rats by increasing IOP with an infusion needle connected to a saline bag. Just before the induction of ischemia, 4  $\mu$ L of 1 mM HPF was given intravitreally, followed by 60 minutes of ischemia. Fifteen minutes after reperfusion, the retinas were flatmounted and imaged in their entirety using a laser confocal-scanning microscope (Fig. 2A). The retinal HPF-fluorescence in the H<sub>2</sub>-loaded eye drop-treated group was significantly less than that in the vehicle-treated group (Fig. 2B).

### Effect of H<sub>2</sub>-Loaded Eye Drops on the Number of Apoptotic and Oxidative Stress Marker-Positive Cells

To determine whether the administration of H<sub>2</sub>-loaded eye drops protects against retinal I/R injury, eye drops with and without H<sub>2</sub> were applied during the entire 90 minutes process (60 minutes of ischemia followed by 30 minutes of reperfusion). One day after I/R injury, a remarkable increase in the number of apoptotic cells (TUNEL-positive cells) was observed in both the inner and the outer nuclear layers of vehicle-treated retinas (Fig. 3A); however, the administration of H<sub>2</sub>-loaded eye drops resulted in a significant decrease (approximately 77%, *P* < 0.0001) of TUNEL-positive cells (Figs. 3A, 3B), indicating that H<sub>2</sub>-loaded eye drops had potent antiapoptotic activity. We speculate that the decreased apoptotic cell death reflects the H<sub>2</sub>-dependent reduction of oxidative stress, which was mainly promoted by  $\cdot$ OH.

We then examined the levels of two oxidative stress markers, 4-HNE and 8-OHdG, in the vehicle-treated and the H<sub>2</sub>-loaded eye drop-treated eyes by immunohistochemical staining with each specific antibody.<sup>30,31</sup> As expected,<sup>9</sup> 1 day after I/R injury, the number of 4-HNE- and 8-OHdG-positive cells increased dramatically in the retina (Figs. 3C, 3E, respectively). However, eyes that had been treated with H<sub>2</sub>-loaded eye drops exhibited significantly fewer 4-HNE and 8-OHdG-positive cells compared with the vehicle-treated retinas (Figs. 3C-F), supporting our formulated hypothesis.

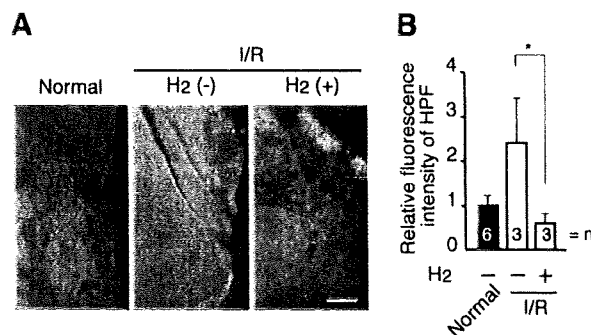
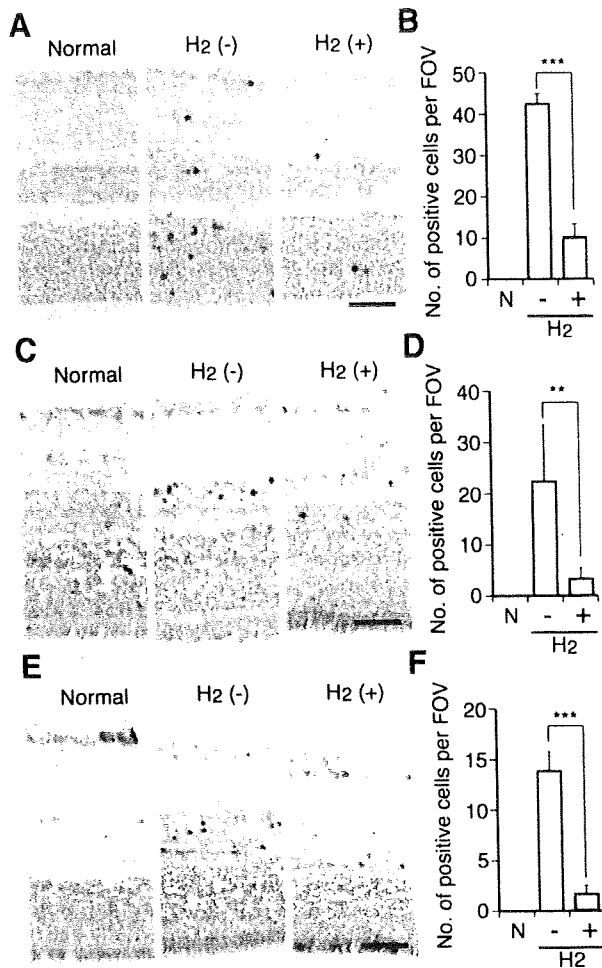


FIGURE 2. H<sub>2</sub>-loaded eye drops reduced hydroxyl radicals in the retina. HPF was given intravitreally just before the induction of ischemia. After I/R, the retinas were quickly removed and flatmounted. (A) Representative fluorescent images were obtained with a laser scanning confocal microscope. (B) HPF fluorescence was quantified from the entire retina of each independent experiment. \**P* < 0.01. Data represent the mean  $\pm$  SD. Scale bar, 200  $\mu$ m.



**FIGURE 3.** H<sub>2</sub>-loaded eye drops reduced apoptotic cell death and oxidative stress. One day after I/R, the eyes were immediately enucleated and fixed for TUNEL assay (A, B) and staining with antibodies against oxidative stress markers +HNE (C, D) and 8-OHdG (E, F). Images of representative slices (A, C, E) and the number of positive cells per field of view (FOV) (B, D, F) in normal retina (N) and the I/R-injured retinas treated with the vehicle (H<sub>2</sub> -) or the H<sub>2</sub>-loaded eye drops (H<sub>2</sub> +) are shown (*n* = 5 animals per group). \*\**P* < 0.001. \*\*\**P* < 0.0001. Data represent the mean ± SD. Scale bar, 30 μm.

**Effect of H<sub>2</sub>-Loaded Eye Drops on Histopathologic and Morphometric Changes**

To further evaluate the protective effect of H<sub>2</sub>-loaded eye drops, we observed histopathologic and morphometric changes 7 days after retinal I/R injury. First, eye drops with and without H<sub>2</sub> were applied during the entire 90-minute process (duration F in Fig. 4A). Histopathologic changes of the retina at 7 days after I/R injury are depicted in Figure 4B. The H<sub>2</sub>-loaded eye drop-treated group showed a nearly normal structure with a thicker retina; however, the H<sub>2</sub>-free (vehicle) eye drops-treated group exhibited a marked thinning and atrophy of the retina. Quantitative morphometry of retinal thickness was used to estimate the effect of H<sub>2</sub> (Fig. 4C). The thickness in the I/R-injured retina treated with the H<sub>2</sub>-loaded eye drops (102.6 ± 3.8 μm) increased significantly compared with the retina treated with the vehicle (66.9 ± 7.8 μm, *P* < 0.0001). In normal retina from untreated animals, the mean thickness of

the retina was 117.0 ± 4.5 μm, indicating that the H<sub>2</sub>-loaded eye drops improved the recovery of retinal thickness by >70%.

To investigate the effect of different durations of H<sub>2</sub>-loaded eye drop administration, we applied H<sub>2</sub>-loaded eye drops using three different time courses (Fig. 4A) and observed that the H<sub>2</sub>-loaded eye drops exerted their effect only when H<sub>2</sub> was already inside the eyeball at the onset of reperfusion (Fig. 4C). There were no significant differences in retinal thickness between groups treated with H<sub>2</sub>-loaded eye drops only after reperfusion (duration R: 75.4 ± 10.4 μm) and treated with

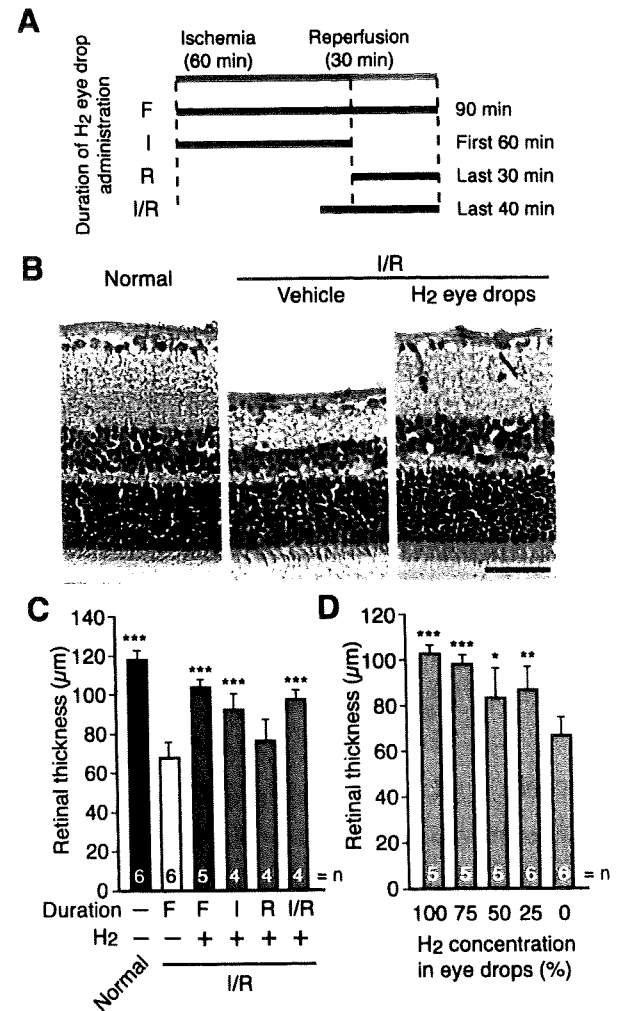


**FIGURE 4.** H<sub>2</sub>-loaded eye drops prevented retinal degeneration caused by I/R. One week after I/R injury, the retinas were sliced and stained with H&E. (A) Schematic of the experiment, with four different durations of H<sub>2</sub>-loaded eye drops administration. (B) Images of representative slices of normal retinas, I/R-injured retinas treated with vehicle, and retinas treated with H<sub>2</sub>-loaded eye drops during the entire 90-minute process (60 minutes of ischemia followed by 30 minutes of reperfusion) are shown. Scale bar, 50 μm. (C) Retinal thicknesses for different durations of H<sub>2</sub>-loaded eye drops (100%) administration. \*\*\**P* < 0.0001 compared with I/R-injured retina treated with the vehicle (H<sub>2</sub> -). (D) Retinal thicknesses at different concentrations of H<sub>2</sub> in eye drops. The retinas were treated with H<sub>2</sub>-loaded eye drops during the entire process (duration F). \**P* < 0.01. \*\**P* < 0.001. \*\*\**P* < 0.0001 compared with I/R-injured retina treated with 0% H<sub>2</sub>. Histograms represent the mean ± SD.

vehicle ( $P = 0.06$ ). However, the retina that was treated with H<sub>2</sub>-loaded eye drops only during ischemia (duration I;  $91.6 \pm 7.5 \mu\text{m}$ ) was still significantly thicker than that treated with the vehicle ( $P < 0.01$ ). We next administered H<sub>2</sub>-loaded eye drops for 10 minutes before and 30 minutes after reperfusion (duration I/R) and observed that the administration schedule was sufficient to suppress the reduction of retinal thickness (duration I/R;  $96.6 \pm 4.4 \mu\text{m}$ ;  $P < 0.001$  vs. vehicle). Furthermore, we applied eye drops diluted to 25%, 50%, and 75% of the normal H<sub>2</sub>-loaded eye drops during the entire 90-minute process and observed that H<sub>2</sub>-loaded eye drops suppressed the reduction of retinal thickness in a dose-dependent manner (Fig. 4D). It is notable that the 25%-diluted H<sub>2</sub>-loaded eye drops were still effective.

### Effect of H<sub>2</sub>-Loaded Eye Drops on Glial Activation

Considering the critical role of increasing glial activation in the pathogenic progression of retinal damage, we investigated the immunohistochemical changes of the Iba1<sup>32</sup> and GFAP<sup>33</sup> at 7 days after retinal I/R injury with and without H<sub>2</sub> treatment. Iba1 is specifically expressed by microglia/macrophages.<sup>34</sup> A small number of Iba1-positive cells was observed in normal retinas, whereas an increasing number of Iba1-positive cells was observed in I/R-injured retinas. At that time, H<sub>2</sub>-loaded eye drops were observed to inhibit the activation of microglia (Figs. 5A, 5B), indicating that the ongoing neurodegeneration, which activated microglia, was repressed by H<sub>2</sub>. In addition, H<sub>2</sub>-loaded eye drops repressed the increase in GFAP immunoreactivity in I/R-injured retinas. The only GFAP-positive cells in normal retina are astrocytes, whereas in the injured retinas, Müller cells, the specific glial cells in the retina, react with anti-GFAP antibody across the retinal layers.<sup>35</sup> In vehicle-treated retinas, GFAP was quite prominent in the Müller cells

across the retinal layers and was also strongly present in the astrocytes of the nerve fiber layers, when compared with the H<sub>2</sub>-loaded eye drop-treated retinas (Fig. 5C).

### DISCUSSION

H<sub>2</sub>-loaded eye drops have a strong protective effect against retinal I/R injury. Previous studies have demonstrated that antioxidants can decrease retinal injury<sup>6-15</sup>; however, because antioxidants are difficult to deliver into the vitreous body by topical administration, they were injected into either the eye or the peritoneal cavity. Thus, easily applicable antioxidative reagents without significant side effects are strongly desirable. H<sub>2</sub> is an antioxidant that can easily diffuse into the body. We have observed that H<sub>2</sub> diffuses into the organelles, including mitochondria and the nucleus, of cultured cells.<sup>18</sup> These properties prompted us to attempt the administration of H<sub>2</sub>-loaded eye drops for retinal diseases. This is the first report that H<sub>2</sub> can immediately penetrate the vitreous body after the administration of H<sub>2</sub>-loaded eye drops, thereby directly reducing a toxic ROS, ·OH, which is produced during I/R. This effectively protects the retina from I/R injury.

Although the sources and mechanisms of ROS generation during I/R by transiently raised IOP are not clearly understood, ROS kills neurons in the ganglion cell layer, inner nuclear layer, and outer nuclear layer mainly by apoptosis.<sup>5,9,35</sup> Ophir et al.<sup>14,15</sup> demonstrated that a burst of ·OH occurs in the cat retina during the early reperfusion phase (5 minutes of reperfusion). Thus, we assessed ·OH after 15 minutes of reperfusion with HPF fluorescence and found that the accumulation of ·OH was reduced by H<sub>2</sub>-loaded eye drops in the I/R-injured retina, indicating that H<sub>2</sub> directly reduced ·OH and decreased subsequent oxidative stress. Indeed, 1 day after reperfusion, H<sub>2</sub>-loaded eye drops dramatically decreased 4-HNE, 8-OHdG, and TUNEL-positive cells indicating that H<sub>2</sub> protected lipids from peroxidation and DNA from oxidation and reduced subsequent retinal cell death (detected as apoptosis) after I/R injury.

Neurodegeneration was obvious at 7 days after retinal I/R injury. Previous studies on retinal damage 7 days after I/R injury have shown that the thinning of the retina was evident both morphologically and morphometrically.<sup>1,26,36,37</sup> In the present study, H<sub>2</sub>-loaded eye drops clearly suppressed the thinning of the retina. However, when H<sub>2</sub>-loaded eye drops were applied after the onset of reperfusion (duration R), they did not protect from retinal damage (Fig. 4). As shown in Figure 1, H<sub>2</sub> concentration in the vitreous body gradually increased after 2 minutes and reached its maximum level after 15 minutes. Immediately after H<sub>2</sub>-loaded eye drop administration was stopped, the H<sub>2</sub> level gradually decreased and then completely disappeared after 15 minutes. Thus, H<sub>2</sub> applied after the onset of reperfusion could not reach a level sufficient to inhibit the accumulation of ·OH in the early reperfusion phase, whereas H<sub>2</sub> applied before or during reperfusion (duration I or I/R) had a high enough H<sub>2</sub> level.

Microglia, Müller cells, and most likely astrocytes respond within hours to elevation of IOP in the retina.<sup>38</sup> Heterogeneous populations of microglia/macrophages are observed in the normal retina and activated early after I/R injury.<sup>39</sup> Dying neurons are phagocytosed by them. The long duration of ROS production (up to 48 hours after I/R) may be explained partly by the infiltration of microglia/macrophages into the site of inflammation.<sup>9</sup> The presence of GFAP in a glial cell is considered a marker for reactive gliosis, which is not neuroprotective, but rather promotes neurodegeneration.<sup>40</sup> H<sub>2</sub>-loaded eye drops reduced the number of reactive glia, indicating that H<sub>2</sub>-loaded eye drops during I/R were sufficient to suppress harmful gliosis after I/R injury and recover the thickness of the retina.

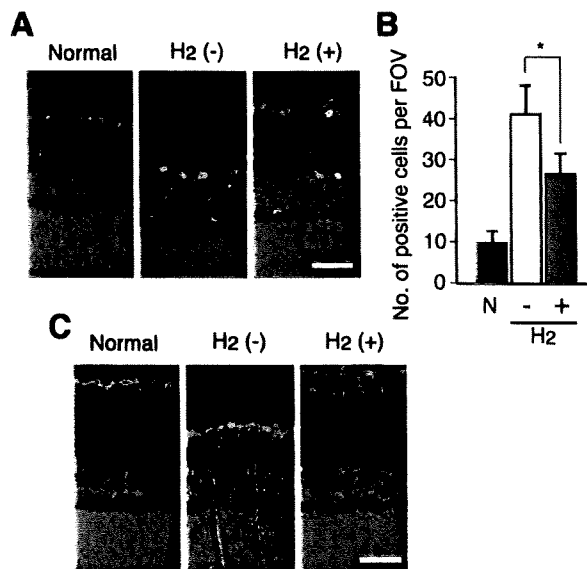


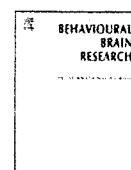
**FIGURE 5.** H<sub>2</sub>-loaded eye drops prevented glial activation caused by I/R in the retina. One week after I/R injury, the retinas were sliced, stained with antibodies to Iba1 (a marker for microglia/macrophages, green) (A, B) and GFAP (a marker for Müller cells and astrocytes, green) (C), and further counterstained for nuclei with propidium iodide (red). Images of representative slices (A, C) and the number of positive cells per field of view (FOV) (B) in normal retina (N) and I/R-injured retinas treated with the vehicle (H<sub>2</sub> -) or H<sub>2</sub>-loaded eye drops (H<sub>2</sub> +) are shown ( $n = 5$  animals per group). \* $P < 0.01$ . Data represent the mean  $\pm$  SD. Scale bar, 50  $\mu\text{m}$ .



In conclusion, this study demonstrates that the topical application of H<sub>2</sub> can be a useful antioxidant to protect against retinal I/R injury by direct H<sub>2</sub> diffusion into the retina. Accordingly, this neuroprotective antioxidant could offer a new therapeutic strategy to the clinical setting to reduce retinal damage in acute glaucoma and acute retinal vascular occlusion.

## References

- Hughes WF. Quantitation of ischemic damage in the rat retina. *Exp Eye Res.* 1991;53:573-582.
- Kuroiwa S, Katai N, Shibuki H, et al. Expression of cell cycle-related genes in dying cells in retinal ischemic injury. *Invest Ophthalmol Vis Sci.* 1998;39:610-617.
- Osborne NN, Casson RJ, Wood JPM, Chidlow G, Graham M, Melena J. Retinal ischemia: mechanisms of damage and potential therapeutic strategies. *Prog Retina Eye Res.* 2004;23:91-147.
- McCord JM. Oxygen-derived free radicals in postischemic tissue injury. *N Engl J Med.* 1985;312:159-163.
- Tezel G. Oxidative stress in glaucomatous neurodegeneration: mechanisms and consequences. *Prog Retinal Eye Res.* 2006;25:490-513.
- Szabo ME, Droy-Lefaix MT, Doly M, Carré C, Braquet P. Ischemia and reperfusion-induced histologic changes in the rat retina. *Invest Ophthalmol Vis Sci.* 1991;32:1471-1478.
- Muller A, Pietri S, Villain M, Frejaville C, Bonne C, Calcasi M. Free radicals in rabbit retina under ocular hyperpressure and functional consequences. *Exp Eye Res.* 1997;64:637-643.
- Shibuki H, Katai N, Kuroiwa S, Kurokawa T, Yodoi J, Yoshimura N. Protective effect of adult T-cell leukemia-derived factor on retinal ischemia-reperfusion injury in the rat. *Invest Ophthalmol Vis Sci.* 1998;39:1470-1477.
- Shibuki H, Katai N, Yodoi J, Uchida K, Yoshimura N. Lipid peroxidation and peroxytrite in retinal ischemia-reperfusion injury. *Invest Ophthalmol Vis Sci.* 2000;41:3607-3614.
- Hirooka K, Miyamoto O, Jinning P, et al. Neuroprotective effects of D-allose against retinal ischemia-reperfusion injury. *Invest Ophthalmol Vis Sci.* 2006;47:1653-1657.
- Zhang B, Safa R, Rusciano D, Osborne NN. Epigallocatechin gallate, an active ingredient from green tea, attenuates damaging influences to the retina caused by ischemia/reperfusion. *Brain Res.* 2007;1159:40-53.
- Peachey NS, Green DJ, Ripps H. Ocular ischemia and the effects of allopurinol on functional recovery in the retina of the arterially perfused cat eye. *Invest Ophthalmol Vis Sci.* 1993;34:58-65.
- Li S, Fu Z, Ma H, et al. Effect of lutein on retinal neurons and oxidative stress in a model of acute retinal ischemia/reperfusion. *Invest Ophthalmol Vis Sci.* 2009;50:836-843.
- Ophir A, Berenshtein E, Kitrossky N, et al. Hydroxyl radical generation in the cat retina during reperfusion following ischemia. *Exp Eye Res.* 1993;57:351-357.
- Ophir A, Berenshtein E, Kitrossky N, Averbukh E. Protection of the transiently ischemic cat retina by zinc-desferrioxamine. *Invest Ophthalmol Vis Sci.* 1994;35:1212-1222.
- Song Y, Gong Y, Xie Z, Li C, Gu Q, Wu X. Edaravone (MCI-186), a free radical scavenger, attenuates retinal ischemia/reperfusion injury in rats. *Acta Pharmacol Sin.* 2008;29:823-828.
- Nakao A, Sugimoto R, Billiar TR, McCurry KR. Therapeutic antioxidant medical gas. *J Clin Biochem Nutr.* 2009;44:1-13.
- Ohsawa I, Ishikawa M, Takahashi K, et al. Hydrogen acts as a therapeutic antioxidant by selectively reducing cytotoxic oxygen radicals. *Nat Med.* 2007;13:688-694.
- Cai J, Kang Z, Liu K, et al. Neuroprotective effects of hydrogen saline in neonatal hypoxia-ischemia rat model. *Brain Res.* 2009;1256:129-137.
- Hayashida K, Sano M, Ohsawa I, et al. Inhalation of hydrogen gas reduces infarct size in the rat model of myocardial ischemia-reperfusion injury. *Biochem Biophys Res Commun.* 2008;373:30-35.
- Fukuda K, Asoh S, Ishikawa M, Yamamoto Y, Ohsawa I, Ohta S. Inhalation of hydrogen gas suppresses hepatic injury caused by ischemia/reperfusion through reducing oxidative stress. *Biochem Biophys Res Commun.* 2007;361:670-674.
- Buchholz BM, Kaczorowski DJ, Suquimoto R, et al. Hydrogen inhalation ameliorates oxidative stress in transplantation induced intestinal graft injury. *Am J Transplant.* 2008;8:2015-2024.
- Nagata K, Nakashima-Kamimura N, Mikami T, Ohsawa I, Ohta S. Consumption of molecular hydrogen prevents the stress-induced impairments in hippocampus-dependent learning tasks during chronic physical restraint in mice. *Neuropsychopharmacology.* 2009;34:501-508.
- Fu Y, Ito M, Fujita Y, et al. Molecular hydrogen is protective against 6-hydroxydopamine-induced nigrostriatal degeneration in a rat model of Parkinson's disease. *Neurosci Lett.* 2009;453:81-85.
- Kajiyama S, Hasegawa G, Asano M, et al. Supplementation of hydrogen-rich water improves lipid and glucose metabolism in patients with type 2 diabetes or impaired glucose tolerance. *Nutr Res.* 2008;28:137-143.
- Lam TT. The effect of 3-aminobenzamide, an inhibitor of poly-ADP-ribose polymerase, on ischemia/reperfusion damage in rat retina. *Res Commun Mol Pathol Pharmacol.* 1997;95:241-252.
- Tomizawa S, Imai H, Tsukada S, et al. The detection and quantification of highly reactive oxygen species using the novel HPF fluorescence probe in a rat model of focal cerebral ischemia. *Neurosci Res.* 2005;53:304-313.
- Setasukinai K, Urano Y, Kakinuma K, Majima HJ, Nagano T. Development of novel fluorescence probes that can reliably detect reactive oxygen species and distinguish specific species. *J Biol Chem.* 2003;278:3170-3175.
- Gavrieli Y, Sherman Y, Ben-Sasson SA. Identification of programmed cell death in situ via specific labeling of nuclear DNA fragmentation. *J Cell Biol.* 1992;119:493-501.
- Petersen DR, Doorn JA. Reactions of 4-hydroxynonenal with proteins and cellular targets. *Free Radic Biol Med.* 2004;37:937-945.
- Kamiya H. Mutagenicities of 8-hydroxyguanine and 2-hydroxyadenine produced by reactive oxygen species. *Biol Pharm Bull.* 2004;27:475-479.
- Imai Y, Ibata I, Ito D, Ohsawa K, Kohsaka S. A novel gene iba1 in the major histocompatibility complex class III region encoding an EF hand protein expressed in a monocytic lineage. *Biochem Biophys Res Commun.* 1996;224:855-862.
- Block F, Grommes C, Kosinski C, Schmidt W, Schwarz M. Retinal ischemia induced by the intraluminal structure method in rats. *Neurosci Lett.* 1997;232:45-48.
- Sasaki Y, Ohsawa K, Kanazawa H et al. Iba1 is an actin-cross-linking protein in macrophages/microglia. *Biochem Biophys Res Commun.* 2001;286:292-297.
- Bonne C, Muller A, Villain M. Free radicals in retinal ischemia. *Gen Pharmacol.* 1998;30:275-280.
- Takahashi K, Lam TT, Edward DP, Buchi ER, Tso MOM. Protective effects of flunarizine on ischemic injury in the rat retina. *Arch Ophthalmol.* 1992;110:862-870.
- Junk AK, Mammis A, Savitz SI, et al. Erythropoietin administration protects retinal neurons from acute ischemia-reperfusion injury. *Proc Natl Acad Sci USA.* 2002;99:10659-10664.
- Wang X, Tay SS, Ng YK. An immunohistochemical study of neuronal and glial cell reactions in retinas of rats with experimental glaucoma. *Exp Brain Res.* 2000;132:476-484.
- Zhang C, Lam TT, Tso MO. Heterogeneous populations of microglia/macrophages in the retina and their activation after retinal ischemia and reperfusion injury. *Exp Eye Res.* 2005;81:700-709.
- Kim K, Ju W, Neufeld AH. Neuronal susceptibility to damage: comparison of the retinas of young, old and old/caloric restricted rats before and after transient ischemia. *Neurobiol Aging.* 2004; 25:491-500.



## Research report

## Oral supplementation with melon superoxide dismutase extract promotes antioxidant defences in the brain and prevents stress-induced impairment of spatial memory

Sanae Nakajima<sup>a</sup>, Ikuroh Ohsawa<sup>a</sup>, Kazufumi Nagata<sup>a</sup>, Shigeo Ohta<sup>a</sup>, Makoto Ohno<sup>b</sup>, Tetsuo Ijichi<sup>c</sup>, Toshio Mikami<sup>d,\*</sup>

<sup>a</sup> Department of Biochemistry and Cell Biology, Institute of Gerontology, Nippon Medical School, Kawasaki, Kanagawa 211-8533, Japan

<sup>b</sup> Department of Graduate School of Nippon Sport Science University, 7-1-1 Fukasawa, Setagaya-ku, Tokyo 158-8508, Japan

<sup>c</sup> Combi Corporation, 5-2-39 Nishibori, Sakura-ku, Saitama-shi, Saitama 338-0832, Japan

<sup>d</sup> Department of Health and Sports Science, Nippon Medical School, 2-297-2 Kosugi-cho, Nakahara-ku, Kawasaki, Kanagawa 211-0063, Japan

## ARTICLE INFO

## Article history:

Received 25 October 2008

Accepted 15 December 2008

Available online 23 January 2009

## Keywords:

GliSODin  
Hippocampus  
Stress  
Memory  
Neurogenesis  
Antioxidant

## ABSTRACT

The purpose of this study was to investigate the effect of antioxidant ingestion on stress-induced impairment of cognitive memory. Male C57BL/6 mice were divided into four groups as follows: (1) control mice (C mice) fed in a normal cage without immobilization; (2) restraint-stressed (RS mice) fed in a small cage; (3) vitamin E mice (VE mice), mice were fed in a small cage with a diet supplemented with vitamin E; (4) GliSODin mice (GS mice) fed in a small cage with a diet supplemented with GliSODin. RS, VE and GS mice were exposed to 12 h of immobilization daily. Five weeks later, spatial learning was measured using the Morris Water Maze (MWM) test. After water maze testing, we performed immunohistochemical analysis using 4-hydroxy-2-nonenal (4-HNE) and an anti-Ki67 antibody. 4-HNE is a marker of lipid peroxidation. RS mice showed impaired spatial learning performance and an increased number of 4-HNE-positive cells in the granule cell layer (GCL) of the hippocampal dentate gyrus when compared to C mice. Moreover, RS mice showed a decreased number of Ki67-positive cells in the subgranular zone (SGZ). GS mice showed better spatial learning memory than RS mice. The number of 4-HNE-positive cells in the GCL of GS mice was significantly less than that of RS mice. The number of Ki67-positive cells in the SGZ of GS mice was significantly greater than that of RS mice. These findings suggest that GliSODin prevents stress-induced impairment of cognitive function and maintains neurogenesis in the hippocampus through antioxidant activity.

© 2008 Elsevier B.V. All rights reserved.

### 1. Introduction

Aging leads to suppression of brain functions such as learning and memory. This effect is accelerated by chronic stress, especially psychological stress. Chronic immobilization stress significantly impaired spatial performance in the MWM, elevated plasma corticosterone levels, and attenuated hippocampal long-term potentiation (LTP) [1]. Escape latencies in the MWM were longer in rats restrained for 21 days than in control rats [2].

Stress-induced impairment of learning and memory is closely related to suppression of hippocampal neurogenesis. Chronic restraint stress resulted in impaired performance in the MWM and a decreased number of BrdU-positive cells in the dentate gyrus [3]. Stress suppresses neurogenesis of dentate gyrus granule neu-

rons, and repeated stress causes remodeling of dendrites in the CA3 region, which is particularly important for memory processing [4].

One of the reasons why stress suppresses hippocampal neurogenesis increased oxidative stress. Fontella et al. [5] reported that repeated restraint stress induced an increase in thiobarbituric acid reactive substance (TBARS) levels and in glutathione peroxidase activity in rats. A relationship between impairment of memory and oxidative stress has been reported. In addition, it has been reported that ingestion of the antioxidant flavanol improved spatial memory retention in adult mammals [6]. However, there have been no reports of protective effects of antioxidant on stress-induced impairment of learning and memory.

In the present study, we investigated whether ingestion of an antioxidant protected against stress-induced impairment of learning and memory. We used two types of antioxidants: GliSODin and  $\alpha$ -tocopherol. GliSODin is superoxide dismutase (SOD) extracted from melons and combined with gliadin. SOD catalyzes the dismutation of superoxide into oxygen and hydrogen peroxide and

\* Corresponding author. Tel.: +81 44 733 3719; fax: +81 44 733 3719.  
E-mail address: [mikami@nms.ac.jp](mailto:mikami@nms.ac.jp) (T. Mikami).

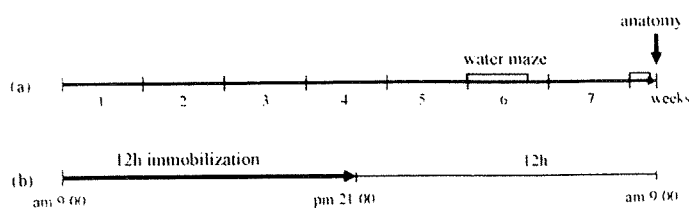


Fig. 1. Experiment protocol: (a) After 5 weeks of chronic immobilization, the spatial memory of all mice was evaluated with the MWM. (b) Chronic immobilization protocol for RA, VE, and GS mice. These mice were exposed to 12 h (9:00 a.m. to 21:00 p.m.) of immobilization in an immobilization cage (width 3 cm, length 3 cm, height 7.5 cm) at a frequency of 6 days per week for 5 weeks. After immobilization, RA, VE and GS mice were fed in six-divided cage. A six-divided cage was made by dividing a standard mouse cage into six sections with plastic boards to make the living space narrow. In this cage, the living space per mouse was 10 cm wide, 10 cm long, and 10.5 cm tall. C mice were fed in a standard mouse cage, where four mice were fed per cage.

is an important antioxidant in nearly all cells exposed to oxygen. In humans, three forms of SOD are present. SOD1 is located in the cytoplasm, SOD2 in the mitochondria, and SOD3 is extracellular. The physiological importance of SODs has been demonstrated by severe pathologies evident in mice genetically engineered to lack these enzymes [7,8]. Additionally, SOD administered as GliSODin led to an increased SOD activity in tissues and protection against oxidative stress. In previous studies, animals supplemented with GliSODin showed significant elevation of circulated antioxidant enzyme activity that was correlated with increased resistance of red blood cells to oxidative stress-induced hemolysis [9]. Supplementation with GliSODin was effective for controlling the thickness of carotid artery intimal and medial layers as measured by ultrasonography-B [10].  $\alpha$ -Tocopherol is also well known to have antioxidant activity. Therefore, we expected that supplementation of GliSODin or  $\alpha$ -tocopherol would enhance the antioxidant capacity of the brain and protect against impairment of learning and memory by chronic stress.

Our findings demonstrate that administration of GliSODin prevented stress-induced impairment of spatial memory, increased the number of Ki67-positive cells, and decreased the number 4-HNE-positive cells. These findings suggest that GliSODin is a useful antioxidant for prevention of stress-induced impairment of cognitive function and neurogenesis in hippocampus.

## 2. Materials and methods

### 2.1. Animals and diet

All experimental procedures and animal treatments were performed in accordance with the guidelines of the laboratory animal manual of Nippon Medical School. Male C57/BL6 mice (Sankyo Lab Service, Tokyo, Japan) aged 7 weeks and weighing  $22.1 \pm 1.3$  g, were used. Mice were randomly divided into four groups: control mice (C mice;  $n = 12$ ), restraint-stressed mice (RS mice;  $n = 10$ ), vitamin E mice (VE mice;  $n = 10$ ), and GliSODin mice (GS mice;  $n = 9$ ). C mice were fed in a standard mice cage (width 32 cm, length 21.5 cm, height 10.5 cm) with standard animal diet (Oriental Yeast Co., Tokyo, Japan). In this case, four mice were fed in a cage. RS mice were fed in a six-divided cage with standard animal diet. The six-divided cage was made from a standard mice cage divided into six partitions with plastic boards to make the living space narrow. In this cage, the living space per mouse was 10 cm wide, 10 cm long, and 10.5 cm tall.

VE and GS mice were fed in the six-divided cage with a standard animal diet supplied with  $\alpha$ -tocopherol or GliSODin, respectively. The VE diet was the standard animal diet supplemented with  $\alpha$ -tocopherol acetate at 88 mg per 100 g of diet to generate an  $\alpha$ -tocopherol intake of 70 mg/(kg day) according to Li et al. [11]. The GliSODin diet was the standard animal diet supplemented with GliSODin at 125 mg per 100 g of diet to generate a GliSODin intake of 100 mg/(kg day) according to Vouldoukis [12]. All mice were fed with ad libitum access to food and water with a 12-h light/dark cycle (24 °C room temperature, 50% humidity).

### 2.2. Immobilization

All mice were acclimatized to the living conditions and diet for 5 days. RS, VE, and GS mice were then exposed to 12 h (9:00 a.m. to 9:00 p.m.) of immobilization in immobilization cage (width 3 cm, length 3 cm, height 7.5 cm) 6 days per week for 5 weeks (Fig. 1). During the daily immobilization period, the mice were only freely able to drink water.

### 2.3. Spatial learning and memory

After 5 weeks of chronic immobilization, the spatial memory of mice was evaluated using the MWM according to the method of Morris with some modifications [13]. Briefly, mice were trained with four trials/day for 5 days. A circular pool that had a diameter of 115 cm was filled with water 1.5 cm above the plastic platform to

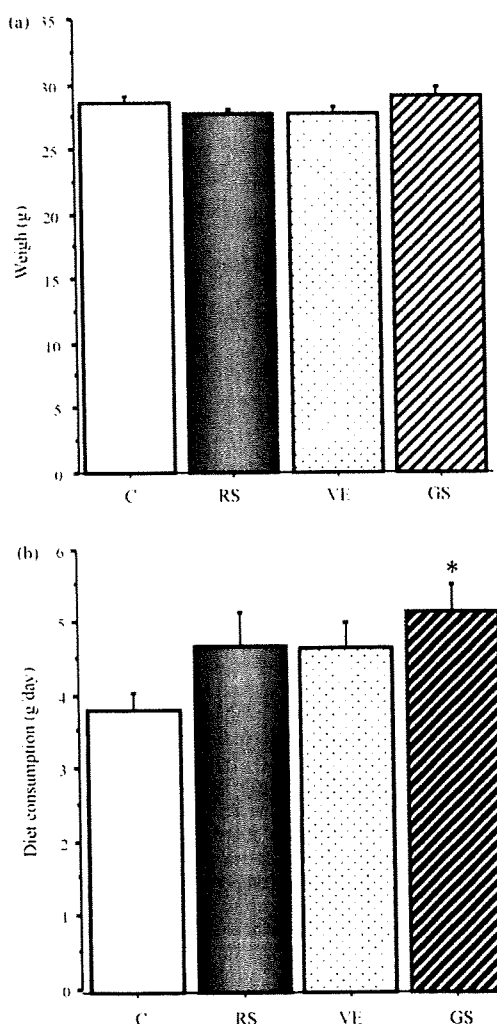


Fig. 2. Body weight and diet consumption: (A) The average weight of mice was not significantly different between conditions. (B) The average diet consumption of RS, VE, and GS mice tended to be greater than that of C mice.

hide it. The water was made opaque with white non-toxic paint and the water temperature was set at 24 °C. A mouse was released into the pool facing the pool wall from four different starting points that were varied randomly each day. The time to reach the platform (escape latency) was recorded for every trial. Each trial lasted either until the mouse had found the platform or for a maximum of 60 s. On each trial, mice were allowed to rest on the platform for 20 s at the end of each trial. To determine long-term retention (memory), the MWM was performed again on the 15th and 16th day after the first MWM.

#### 2.4. Sample collection

The day after completion of MWM, mice were anesthetized with pentobarbital and transcardially perfused with 60 ml saline via the left ventricle. Brains were carefully removed and hemispheres were separated. The left hemisphere was fixed in 4% paraformaldehyde in 0.1 M phosphate-buffered saline (PBS; 137 mM NaCl, 8.10 mM Na<sub>2</sub>HPO<sub>4</sub>, 2.68 mM KCl, 1.47 mM KH<sub>2</sub>PO<sub>4</sub>, pH 7.4) overnight at room temperature. After washing three times with PBS, the brain was cut rostrally at bregma –1.30 mm, caudally at bregma –5.80 mm, and ventrally at 4.5 mm. The areas were serially sectioned rostro-caudally with a Leica vibratome (VT 1000S, Leica Microsystems, Germany) at 50 µm and immersed free-floating in PBS. Ninety-six-well plates were used to keep the sections separate to preserve the order of the series in PBS at 4 °C. The right hemisphere was divided into hippocampus, cerebral cortex, hypothalamus and cerebellum. These samples were quickly frozen with liquid nitrogen and stored at –80 °C until analysis.

#### 2.5. Ki67 immunohistochemistry

To investigate neurogenesis in hippocampus, Ki67-positive cells were identified immunohistochemically. A one-in-eight series of sections (400 µm apart) of every animal was used for stereology of cell counts. The sections were incubated with 3% hydrogen peroxide in methanol to block endogenous peroxidase activity and with normal goat serum to block non-specific staining. After washing with PBS, the sections were exposed to heat (100 °C) in 100 mM citric acid buffer (pH 6.0) for 5 min using a microwave for antigen retrieval. After washing with PBS, the sections were incubated with rabbit polyclonal anti-Ki67 antibody (Abcam, 1:500) for two nights at 4 °C with gentle shaking. After washing with PBS, the sections were incubated with goat anti-rabbit biotinylated IgG (Vector Laboratories, 1:100) for 1 h at room temperature. After washing with PBS, the sections were incubated with avidin-biotin-horseradish peroxidase complex (VECTASTAIN ABC reagent, Vector Laboratories) for 2 h at room temperature. Finally, the sections were washed in PBS and developed using 0.67 mg/ml 3,3'-diaminobenzidine (DAB) for 5 min.

#### 2.6. 4-HNE immunohistochemistry

To investigate lipid peroxidation in hippocampus, 4-HNE immunohistochemistry was performed using M.O.M. immunodetection kit (Vector laboratory, USA) according to the manufacturer's instructions. A one-in-eight series of sections (400 µm apart) of every animal was used for stereology of cell counts. Briefly, free-floating sections were washed in PBS and reacted with 3% hydrogen peroxide in methanol for 30 min to block endogenous peroxidase activity. After washing with PBS, the sections were treated as described above for antigen retrieval. After washing with PBS, the sections were incubated with M.O.M. mouse IgG blocking solution for 1 h. After washing with PBS, the sections were incubated with 10 µg/ml of monoclonal anti-4-HNE antibody (Japan Institute for the Control of Aging, Japan) in M.O.M. diluent (0.1 M PBS; pH 7.4, 0.5% Triton X-100, 8% protein concentrate stock solution) for two nights at 4 °C with gentle shaking. After washing with PBS, the sections were incubated with biotinylated anti-mouse IgG in M.O.M. diluent (1:250) for 2 h at room temperature. After washing with PBS, the sections were incubated with avidin-biotin-horseradish peroxidase complex for 2 h at room temperature. Finally, the sections were then incubated with VECTASTAIN ABC reagent (Vector Laboratories) for 1 h and developed using DAB.

The sections reacted with Ki67 or 4-HNE antibodies were mounted, dehydrated, and coverslipped using Permount mounting medium. For stereology, Ki67-positive cells and 4-HNE-positive cells were counted in subgranular zone (SGZ) or granule cell layer (GCL) using a light microscope (ECLIPSE E400 Nikon; Nikon, Japan) with a 40× objective (Nikon).

#### 2.7. Analysis of SOD activity and $\alpha$ -tocopherol content

SOD activity was measured using the SOD Assay Kit-WST (Dojindo Molecular Technologies Co., Tokyo) as follows: 20 mg of hippocampus was homogenized in the dilution buffer included in the SOD assay kit and centrifuged at 18,000 × g for 10 min. The protein concentration of the supernatant was measured using Coomassie Plus Protein Assay Reagent Kit (Pierce Co., Ltd.). The supernatant (20–50 µg protein) was used for measurement of SOD activity in accordance with the manufacturer's instructions. SOD activity was expressed as SOD content per gram total protein (units/g protein). The level of  $\alpha$ -tocopherol in hypothalamus was determined by high performance liquid chromatography (HPLC) according to the method of Milne and Botnen with some modifications [14]. We used the hypothalamus for  $\alpha$ -tocopherol

analysis because the hippocampus and cerebral cortex had already been used for other analyses.

#### 2.8. Statistical analysis

Data are presented as mean ± S.E. Statistical analysis was performed using Fisher's PLSD post hoc test.  $p < 0.05$  was accepted as significant.

### 3. Results

#### 3.1. Weight and diet consumption

Chronic immobilization and feeding in the six-divided cage did not result in any differences in body weight between groups (Fig. 2A). However, the diet consumption of RS, VE, and GS mice tended to be greater than that of C mice (Fig. 2B).

#### 3.2. Learning and memory

To examine whether stressful conditions (12 h immobilization and feeding in a narrow space) would influence cognitive performance, we tested both learning and memory (Fig. 3). In learning, control mice showed a reduced latency for finding the hidden platform during 5 days of training, whereas RS mice had a significantly longer latency than C mice on days 4 and 5 during the training period ( $p < 0.05$ ). This finding confirms that the experimental conditions used in the present study were stressful enough to impair the learning of RS mice. On the other hand, GS mice showed a latency reduction equal to that of C mice and had a significantly shorter latency than RS mice on day 5 ( $p < 0.05$ ), whereas VE mice did not show a latency reduction equal to that of C mice.

To test memory, mice were exposed to the MWM again on days 15 and 16 (Fig. 3). Both C and GS mice remembered the position of the platform well and showed a latency reduction between days 15 and 16, whereas RS mice had a significantly longer latency than C and GS mice and did not improve. VE mice showed reduced latency but still showed a significantly longer latency than C and GS mice.

#### 3.3. 4-HNE-positive cells in the GCL of the dentate gyrus

Previous studies have shown that psychological stress leads to increased lipid peroxidation in the brain [15]. However, these findings were based on analyses of brain homogenate; no study has actually shown the localization of lipid peroxide in the hippocam-

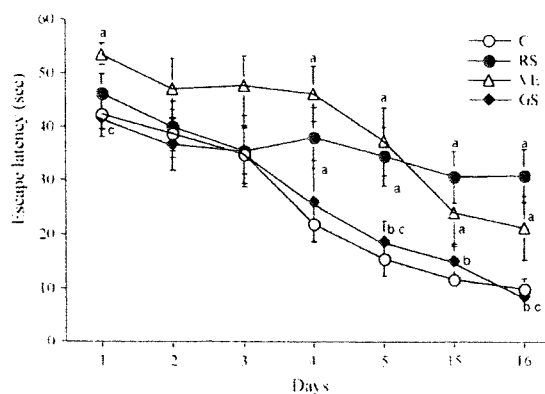
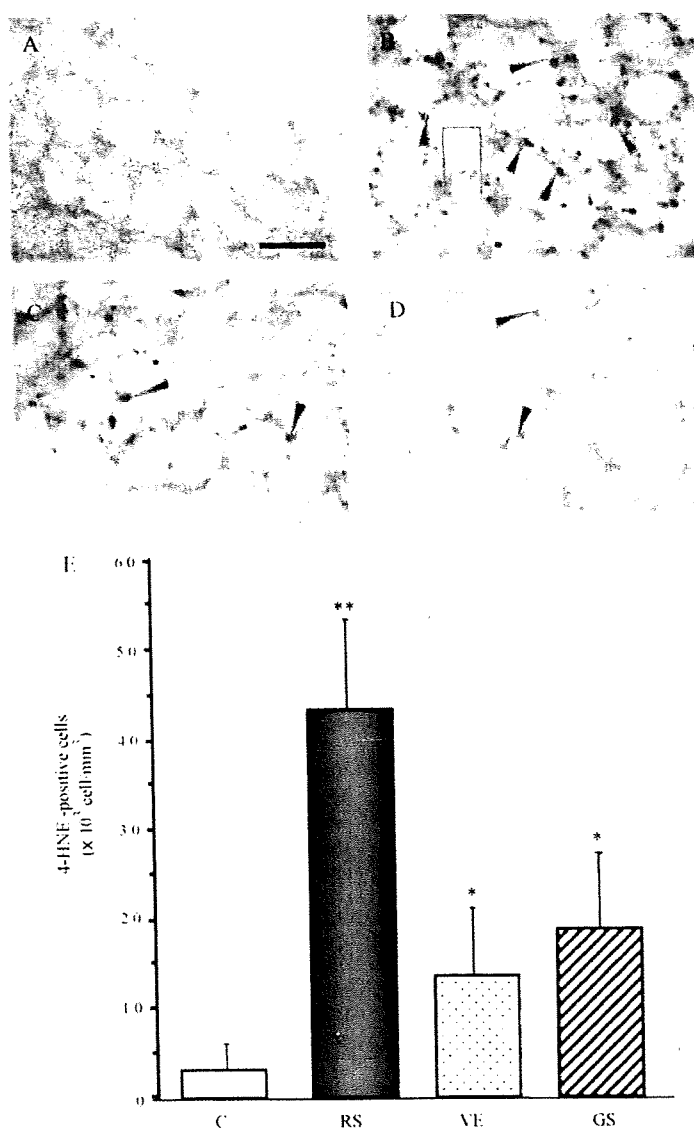


Fig. 3. Spatial learning and memory as measured by MWM. RS mice showed significantly impairment of escape latency when compared to C mice. However, the escape latency of GS mice was significantly shorter than that of the RA group. Significant differences in escape latency between the RS and GS group were also maintained on days 15 and 16. The data are shown as the mean ± S.E. (a)  $p < 0.05$  vs. C mice, (b)  $p < 0.05$  vs. RS mice, (c)  $p < 0.05$  vs. VE mice.



**Fig. 4.** Number of 4-HNE-positive cells in the GCL. Representative images of 4-HNE-positive cells in GCL are shown. (A) C mice, (B) RS mice, (C) VE mice, and (D) GS mice. Bar: 50  $\mu$ m. (E) Total number of 4-HNE-positive cells in the SGZ. RS mice had significantly more 4-HNE-positive cells in the GCL of the dentate gyrus than C mice. GS and VE mice had significantly less 4-HNE-positive cells in the GCL of the dentate gyrus than RS mice. The data are shown as the mean  $\pm$  S.E. (a)  $p < 0.05$  vs. C mice and (b)  $p < 0.05$  vs. RS mice.

pus. Therefore, we used immunohistochemistry to determine whether lipid peroxide was produced in hippocampal neurons under our experimental conditions. As shown in Fig. 4, RS mice had significantly more 4-HNE-positive cells in the dentate gyrus than C mice. GS and VE mice had significantly fewer 4-HNE-positive cells in the dentate gyrus than RS mice. These findings suggest that the stress condition used in the present study caused increased lipid peroxidation in the dentate gyrus and that supplementation with of antioxidants prevented lipid peroxidation induced by chronic stress.

### 3.4. Neurogenesis in the dentate gyrus

To examine whether the beneficial effects of GliSODin on learning and memory could be mediated by increased neurogenesis in

the hippocampus, we measured the number of Ki67-positive cells in the hippocampal dentate gyrus. The number of Ki67-positive cells in the SGZ of the dentate gyrus was significantly lower in RS mice than in control mice (Fig. 5). However, the number of Ki67-positive cells in GS mice was equal to that in C mice and significantly higher than that of RA mice. VE mice did not have an equal number of Ki67-positive to C mice.

### 3.5. SOD activity and $\alpha$ -tocopherol content

We examined the effects of GliSODin and  $\alpha$ -tocopherol administration on SOD activity and  $\alpha$ -tocopherol content in the brain. The mouse hippocampus was too small to measure  $\alpha$ -tocopherol content. Therefore, we used the hypothalamus to measure  $\alpha$ -tocopherol content in the brain.

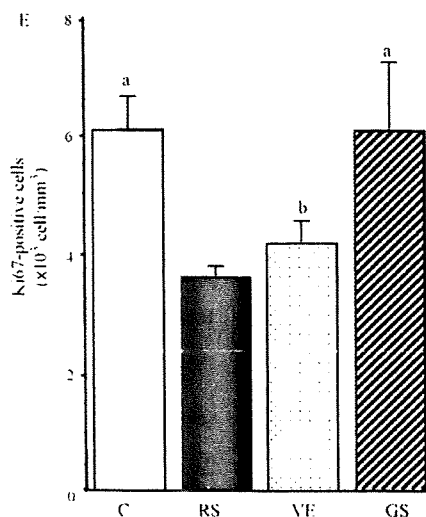
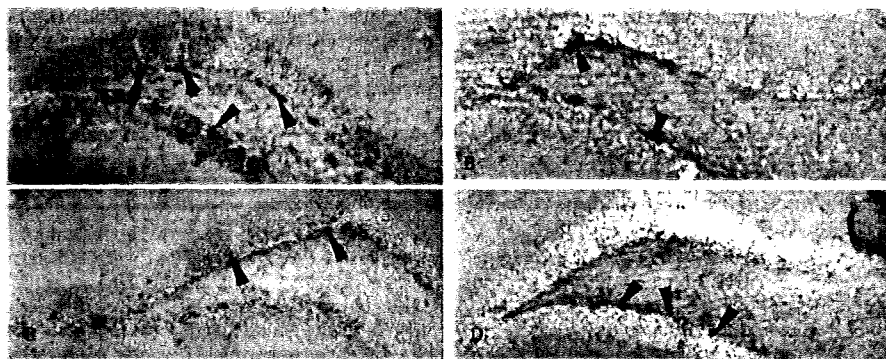


**Fig. 5.** Number of Ki67-positive cells in the SGZ. Representative pictures of Ki67-positive cells in the SGZ are shown. (A) C mice, (B) RS mice, (C) VE mice, (D) GS mice, and (E) Total number of Ki67-positive cells in the SGZ. The number of Ki67-positive cells in the SGZ was significantly lower in RS mice than in C and GS mice. (a)  $p < 0.05$  vs. RA mice and (b)  $p < 0.05$  vs. C mice.

The hippocampal SOD activity of GS mice was significantly greater than that of the other three groups of mice ( $p < 0.05$ ) (Fig. 6A). There was no significant difference in hippocampal SOD activity among C, RS, and VE mice.

RS mice showed a significantly lower content of  $\alpha$ -tocopherol in the hypothalamus compared with control mice (Fig. 6B). In spite of  $\alpha$ -tocopherol administration,  $\alpha$ -tocopherol content in VE mice did not significantly increase when compared to C mice. On the other

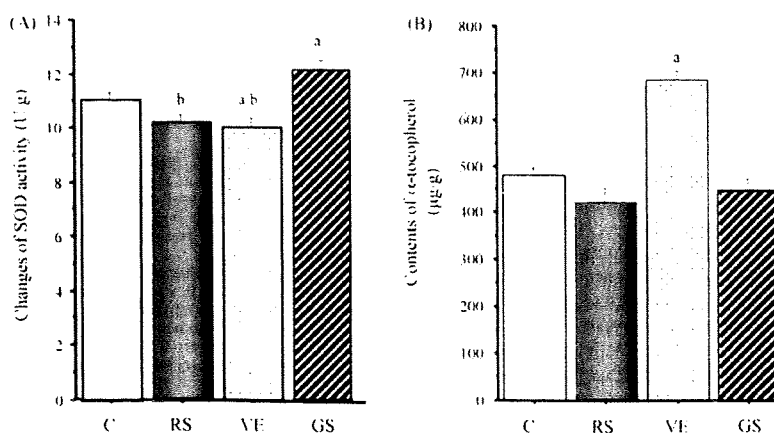


**Fig. 6.** SOD activity and  $\alpha$ -tocopherol content in the brain: (A) SOD activity in hippocampus; SOD activity of GS mice was significantly increased when compared to other mice. (a)  $p < 0.05$  vs. C mice and (b)  $p < 0.05$  vs. GS mice. (B)  $\alpha$ -tocopherol content of the hypothalamus.  $\alpha$ -Tocopherol content of VE mice was significantly increased when compared to other mice. (a)  $p < 0.05$  vs. C mice.

hand, although GS mice were fed a diet with the same amount of  $\alpha$ -tocopherol as the standard diet, they showed a significant higher content of  $\alpha$ -tocopherol than C mice.

#### 4. Discussion

To investigate whether administration of antioxidants improves stress-induced cognitive memory impairment, spatial memory in mice exposed to chronic immobilization and feeding in narrow cages was determined using the MWM after administration of the antioxidants GliSODin and vitamin E. Chronic immobilization and feeding in narrow cages resulted in suppression of spatial memory. In addition, the stressful environment resulted in increased and decreased numbers of 4-HNE-positive and Ki67-positive cells in the dentate gyrus, respectively. Administration of GliSODin prevented the impairment of spatial memory, the reduced number of Ki67-positive cells, and the increased number of 4-HNE-positive cells, whereas administration of vitamin E did not prevent the impairment of spatial memory or the loss of Ki67-positive cells in spite of preventing the increase in 4-HNE-positive cells. These findings suggest that GliSODin prevents stress-induced impairment of cognitive function by suppressing of oxidative stress and maintaining neurogenesis in the hippocampus.

In the present study, mice were fed in narrow cages with 12 h of immobilization to generate psychological stress. Unpredictably, the body weight of mice exposed to stress was not significantly different from C mice. On the other hand, the daily food intake of stressed mice tended to be greater than that of C mice. Chronic stress increases daily food intake of animals [16]. In other experiments, we have investigated plasma corticosterone concentrations in mice exposed to same stressful conditions as in the present study. On the third day after initiation of stressful conditions, the plasma corticosterone concentration was significantly higher than at the pre-stress state (data not shown). Therefore, it is likely that the conditions used in the present study resulted in a stress response.

In the present study, restraint stress impaired spatial memory as measured by the Morris MWM, which corresponded to previous findings [2]. However, mice exposed to restraint stress who received GliSODin did not show impairment of spatial memory (Fig. 3). Decreased hippocampal neurogenesis can impair spatial memory [17]. Chronic restraint stress impaired performance in the MWM and decreased the number of BrdU-positive cells in the dentate gyrus of the hippocampus [3]. In addition, impairment of spatial memory is negatively correlated with hippocampal neurogenesis [18]. Some factors such as environmental enrichment or habitual exercise can increase the number of BrdU-positive cells in the dentate gyrus of hippocampus and in turn enhance spatial memory [19]. In the present study, GliSODin treatment prevented impairment of spatial memory and loss of Ki67-positive cells in the dentate gyrus of hippocampus (Figs. 3 and 5). An increased number of Ki67-positive cells in the dentate gyrus reflects increased hippocampal neurogenesis [20]. Therefore, our findings suggest that GliSODin prevents stress-induced suppression of spatial memory by maintaining hippocampal neurogenesis.

Increase of oxidative stress in the hippocampus also suppresses hippocampal neurogenesis during chronic restraint stress [2,5,21–23]. Repeated restraint stress induced an increase in TBARS levels and glutathione peroxidase activity in rats [5]. Chronic restraint stress also significantly elevated the levels of nitrites and TBARS in the frontal cortex and hippocampus [2]. In the present study, we showed that chronic restraint stress increased the number of 4-HNE-positive cells in the GCL of the dentate gyrus. In addition, our findings show that GliSODin treatment reduced the number of 4-HNE-positive cells (Fig. 4). 4-HNE is a representative oxidative stress marker that specifically labels lipid peroxidation

in cellular membranes [24]. GliSODin treatment simultaneously increased SOD activity in the hippocampus and decreased the number of 4-HNE-positive cells (Fig. 6A). Therefore, GliSODin might prevent lipid peroxidation in hippocampus by increasing hippocampal SOD activity.

In the present study, we investigated the effects of GliSODin and  $\alpha$ -tocopherol on stress-induced lipid peroxidation and impairment of spatial memory. Both GliSODin and  $\alpha$ -tocopherol protected against lipid peroxidation; however GliSODin also prevented impairment of spatial memory. The reason for this discrepancy is unclear; however we speculate that GliSODin treatment may have upregulated neurotrophic factors such as insulin-like growth factor 1 (IGF-1), or nerve growth factor (NGF) in the brain or other tissues. IGF-1 enhances hippocampal neurogenesis and protects against stress-induced impairment of spatial memory [25]. In the intestine, macrophages regard GliSODin as non-self and attacked it by releasing reactive oxygen, resulting in the release of NO into the blood. This NO is transferred to the tissues and stimulates induction of several proteins such as SOD and catalase [12]. In addition, NO induces stimulates induction of IGF-1 [26]. In the present study, GliSODin induced SOD activity in hippocampus (Fig. 6). However, whether GliSODin actually induces expression of neurotrophic factors was not determined in the present study. Further investigations are necessary to elucidate this point. Collectively, our findings suggest that GliSODin prevents stress-induced impairment of cognitive function by preventing lipid peroxidation and maintaining neurogenesis in hippocampus.

#### References

- [1] Daniel TR, Laurie MB, James M, Timothy JT. BDNF protects against stress-induced impairments in spatial learning and memory and LTP. *Hippocampus* 2005;15:246–53.
- [2] Abidin I, Yargicoglu P, Agar A, Gumuslu S, Aydin S, Ozturk O, et al. The effect of chronic restraint stress on spatial learning and memory: relation to oxidant stress. *Int J Neurosci* 2004;114:683–99.
- [3] Bartolomucci A, de Biurrun G, Czeh B, van Kampen M, Fuchs E. Selective enhancement of spatial learning under chronic psychosocial stress. *Eur J Neurosci* 2002;15:1863–6.
- [4] McEwen BS, Magarinos AM, Reagan LP. Structural plasticity and tianeptine: cellular and molecular targets. *Eur Psychiatry* 2002;17(Suppl. 3):318–30.
- [5] Fontella FU, Siqueira IR, Vasconcelos AP, Tabajara AS, Netto CA, Dalmaiz C. Repeated restraint stress induces oxidative damage in rat hippocampus. *Neurochem Res* 2005;30:105–11.
- [6] van Praag H, Lucero MJ, Yeo GW, Stecker K, Heivand N, Zhao C, et al. Plant-derived flavanol(–)epicatechin enhances angiogenesis and retention of spatial memory in mice. *J Neurosci* 2007;27:5869–78.
- [7] Elchuri S, Oberley TD, Qi W, Eisenstein RS, Jackson Roberts L, Van Remmen H, et al. CuZnSOD deficiency leads to persistent and widespread oxidative damage and hepatocarcinogenesis later in life. *Oncogene* 2005;24:367–80.
- [8] Muller FL, Song W, Liu Y, Chaudhuri A, Pieke-Dahl S, Strong R, et al. Absence of CuZn superoxide dismutase leads to elevated oxidative stress and acceleration of age-dependent skeletal muscle atrophy. *Free Radic Biol Med* 2006;40:1993–2004.
- [9] Vouldoukis I, Conti M, Krauss P, Kamate C, Blazquez S, Tefit M, et al. Supplementation with gliadin-combined plant superoxide dismutase extract promotes antioxidant defences and protects against oxidative stress. *Phytother Res* 2004;18:957–62.
- [10] Cloarec M, Caillard P, Provost JC, Dever JM, Elbeze Y, Zamaria N. GliSODin, a vegetal sod with gliadin, as preventative agent vs. atherosclerosis, as confirmed with carotid ultrasound-B imaging. *Allerg Immunol (Paris)* 2007;39:45–50.
- [11] Li R-K, Sole MJ, Mickle DAG, Schimmer J, Goldstein D. Vitamin E and oxidative stress in the heart of the cardiomyopathic syrian hamster. *Free Radic Biol Med* 1998;24:252–8.
- [12] Vouldoukis I, Marc C, Pascal K, Caroline K, Samantha B, Maurel T, Dominique M, Alphonse C, Bernard D. Supplementation with gliadin-combined plant superoxide dismutase extract promotes antioxidant defences and protects against oxidative stress. *Phytother Res* 2004;18:957–62.
- [13] Morris R. Developments of a water-maze procedure for studying spatial learning in the rat. *J Neurosci Methods* 1984;11:47–60.
- [14] Milne DB, Botnen J. Retinol, alpha-tocopherol, lycopene, and alpha- and beta-carotene simultaneously determined in plasma by isocratic liquid chromatography. *Clin Chem* 1986;32:874–6.
- [15] Matsumoto K, Yobimoto K, Huong NTT, Abdel-Fattah M, Van Hien T, Watanabe H. Psychological stress-induced enhancement of brain lipid peroxidation via nitric oxide systems and its modulation by anxiolytic and angiogenic drugs in mice. *Brain Res* 1999;839:74–84.

- [16] Torres SJ, Nowson CA. Relationship between stress, eating behavior, and obesity. *Nutrition* 2007;23:887–94.
- [17] Ibi D, Takuma K, Koike H, Mizoguchi H, Tsuritani K, Kuwahara Y, et al. Social isolation rearing-induced impairment of the hippocampal neurogenesis is associated with deficits in spatial memory and emotion-related behaviors in juvenile mice. *J Neurochem* 2008;105:921–32.
- [18] Nilsson M, Perfilieva E, Johansson V, Orwar O, Eriksson PS. Enriched environment increases neurogenesis in the adult rat dentate gyrus and improves spatial memory. *J Neurobiol* 1999;39:569–78.
- [19] Gobbo OL, O'Mara SM. Exercise, but not environmental enrichment, improves learning after kainic acid-induced hippocampal neurodegeneration in association with an increase in brain-derived neurotrophic factor. *Behav Brain Res* 2005;159:21–6.
- [20] Drapeau E, Mayo W, Arousseau C, Le Moal M, Piazza PV, Abrous DN. Spatial memory performances of aged rats in the water maze predict levels of hippocampal neurogenesis. *Proc Natl Acad Sci* 2003;100:14385–90.
- [21] Grillo CA, Piroli GG, Rosell DR, Hoskin EK, McEwen BS, Reagan LP. Region specific increases in oxidative stress and superoxide dismutase in the hippocampus of diabetic rats subjected to stress. *Neuroscience* 2003;121:133–40.
- [22] Pajovic SB, Pejic S, Stojiljkovic V, Gavrilovic L, Dronjak S, Kanazir DT. Alterations in hippocampal antioxidant enzyme activities and sympatho-adrenomedullary system of rats in response to different stress models. *Physiol Res* 2006;55:453–60.
- [23] Reagan LP, Magarinos AM, Yee DK, Swzeda LI, Van Bueren A, McCall AL, et al. Oxidative stress and HNE conjugation of GLUT3 are increased in the hippocampus of diabetic rats subjected to stress. *Brain Res* 2000;862:292–300.
- [24] Esterbauer H, Schaur RJ, Zollner H. Chemistry and biochemistry of 4-hydroxynonenal, malonaldehyde and related aldehydes. *Free Radic Biol Med* 1991;11:81–128.
- [25] Carro E, Trejo JL, Busiguina S, Torres-Aleman I. Circulating insulin-like growth factor I mediates the protective effects of physical exercise against brain insults of different etiology and anatomy. *J Neurosci* 2001;21:5678–84.
- [26] Chen MJ, Ivy AS, Russo-Neustadt AA. Nitric oxide synthesis is required for exercise-induced increases in hippocampal BDNF and phosphatidylinositol 3' kinase expression. *Brain Res Bull* 2006;68:257–68.





## Hypothesis

## Are the effects of $\alpha$ -glucosidase inhibitors on cardiovascular events related to elevated levels of hydrogen gas in the gastrointestinal tract?

Yoshihiko Suzuki<sup>a</sup>, Motoaki Sano<sup>c,\*</sup>, Kentaro Hayashida<sup>c</sup>, Ikuroh Ohsawa<sup>a,b</sup>, Shigeo Ohta<sup>a</sup>, Keiichi Fukuda<sup>c</sup>

<sup>a</sup>Department of Biochemistry and Cell Biology, Institute of Development and Aging Science, Graduate School of Medicine, Nippon Medical School, Kawasaki City 211-8533, Japan

<sup>b</sup>The Center of Molecular Hydrogen Medicine, Institute of Development and Aging Science, Graduate School of Medicine, Nippon Medical School, Kawasaki City 211-8533, Japan

<sup>c</sup>Department of Regenerative Medicine and Advanced Cardiac Therapeutics, Keio University School of Medicine, Tokyo 160-8582, Japan

## ARTICLE INFO

## Article history:

Received 20 April 2009

Revised 28 May 2009

Accepted 31 May 2009

Available online 6 June 2009

Edited by Quan Chen

## Keywords:

$\alpha$ -Glucosidase inhibitors

Type 2 diabetes

Hydrogen gas

Antioxidant

## ABSTRACT

The major side-effect of treatment with  $\alpha$ -glucosidase inhibitors, flatulence, occurs when undigested carbohydrates are fermented by colonic bacteria, resulting in gas formation. We propose that the cardiovascular benefits of  $\alpha$ -glucosidase inhibitors are partly attributable to their ability to neutralise oxidative stress via increased production of H<sub>2</sub> in the gastrointestinal tract. Acarbose, which is an  $\alpha$ -glucosidase inhibitor, markedly increased H<sub>2</sub> production, with a weaker effect on methane production. Our hypothesis is based on our recent discovery that H<sub>2</sub> acts as a unique antioxidant, and that when inhaled or taken orally as H<sub>2</sub>-dissolved water it ameliorates ischaemia–reperfusion injury and atherosclerosis development.

© 2009 Federation of European Biochemical Societies. Published by Elsevier B.V. All rights reserved.

## 1. Introduction

A growing body of evidence supports the notion that postprandial hyperglycaemia plays an important role in the development of cardiovascular disease. Large epidemiological studies have shown that the serum glucose concentration 2 h after an oral glucose challenge is a powerful predictor of cardiovascular risk [1,2].

$\alpha$ -Glucosidase inhibitors are pharmacological agents that specifically reduce postprandial hyperglycaemia through retardation of disaccharide digestion, thereby reducing glucose absorption by the small intestine. The STOP-NIDDM trial demonstrated that the treatment of patients who had impaired glucose tolerance with the  $\alpha$ -glucosidase inhibitor acarbose was associated with a 25% reduction in the risk of progression to diabetes, a 34% reduction in the risk of developing *de novo* hypertension, and a 49% risk reduction for cardiovascular events [3]. Furthermore, a meta-analysis of seven long-term studies suggested that acarbose reduced the risk of myocardial infarction for patients with type 2 diabetes [4]. Such risk reduction for coronary heart disease events in patients with type 2 diabetes was not observed by the improved glycaemic control achieved with intensified treatment with insulin and glibenclamide [5]. Inhibition of postprandial hyperglycaemia

by  $\alpha$ -glucosidase inhibitors alleviates cardiac ischaemia–reperfusion injury in mice [6]. These findings suggest that  $\alpha$ -glucosidase inhibitors interfere with the development of macrovascular diseases through additional mechanisms distinct from the expected modulation of postprandial hyperglycaemia.

2. Molecular hydrogen (H<sub>2</sub>) acts as a novel antioxidant

Clinical evidence and experimental results strongly implicate reactive oxygen species (ROS) as the leading etiologic agent of cardiovascular diseases, including hypertension, atherosclerosis, angina pectoris, myocardial infarction, and heart failure [7,8]. The mechanisms for ROS production are diverse, and include increases in the activities of NAD(P)H-oxidase, xanthine oxidase, cyclooxygenase, and lipoxygenase, as well as uncoupling of nitric oxide synthase, dysfunction of the mitochondrial respiratory chain, and decreased bioavailability of antioxidants, all of which contribute to increased oxidative stress. An increase in ROS production reduces the bioavailability of nitric oxide (NO), synergistically advancing the pathogenesis of cardiovascular disease, since NO plays important roles in the regulation of vascular tone, inhibition of platelet aggregation, and suppression of smooth muscle cell (SMC) proliferation. Increases in the renal levels of ROS raise the blood pressure by influencing afferent arteriolar tone, tubulo-glomerular feedback response, and sodium reabsorption [9]. Increases in vascular ROS promote endothelial dysfunction, increased

\* Corresponding author. Address: Department of Regenerative Medicine and Advanced Cardiac Therapeutics, Keio University School of Medicine, 35 Shinanomachi Shinjuku-ku, Tokyo 160-8582, Japan. Fax: +81 3 5363 3875.

E-mail address: [msano@sc.itc.keio.ac.jp](mailto:msano@sc.itc.keio.ac.jp) (M. Sano).

contractility, monocyte invasion, VSMC proliferation, and increased deposition of extracellular matrix proteins, all of which contribute to the pathogenesis of hypertension, atherosclerosis, and plaque rupture. In the brain, increased production of ROS mediates hypertension by increasing sympathetic outflow. Various antioxidants have been tested for their abilities to reduce the risk of cardiovascular disease. However, these trials have not verified the importance of antioxidants in the prevention of cardiovascular disease [10]. These outcomes can be partially explained by the dual roles of ROS. Most of the detrimental effects of ROS are attributed to  $\cdot\text{OH}$ , which is the most reactive oxygen species. In comparison,  $\text{O}_2^{\cdot-}$  and  $\text{H}_2\text{O}_2$  have lower oxidative energies and, paradoxically, are implicated as crucial signalling components in the establishment of favourable tolerance to oxidative stress. Consequently, the inhibition of both these pathways (e.g., by antioxidants) can have a deleterious outcome.

Recently, we discovered that molecular hydrogen ( $\text{H}_2$ ) acts as an antioxidant with the following interesting properties: (i)  $\text{H}_2$  permeates cell membranes and can target the cellular organelles, including the mitochondria and nuclei; and (ii)  $\text{H}_2$  specifically quenches detrimental ROS, such as  $\cdot\text{OH}$  and peroxynitrite ( $\text{ONOO}^-$ ), while maintaining the metabolic oxidation–reduction reaction and other less-potent ROS, such as  $\text{O}_2^{\cdot-}$ ,  $\text{H}_2\text{O}_2$  and nitric oxide ( $\text{NO}$ ) [11]. We showed that inhalation of  $\text{H}_2$  gas, given at an incombustible level, limited the extent of myocardial infarction resulting from myocardial ischaemia–reperfusion injury, thereby preventing deleterious left ventricular remodelling in the rat [12]. Importantly, the inhaled  $\text{H}_2$  gas was transported rapidly in the circulation and reached the ‘at-risk’ ischaemic myocardium before the coronary blood flow of the occluded infarct-related artery was re-established.

$\text{H}_2$  can also be administered orally in the form of  $\text{H}_2$ -dissolved water. Kajiyama et al. reported that supplementation with 900 ml/day (300 ml given three times a day) of  $\text{H}_2$ -dissolved water for 8 weeks reduced the levels of several biomarkers of oxidative stress, such as plasma oxidized low-density lipoprotein (LDL) cholesterol and urinary 8-isoprostanes, and improved glucose metabolism in patients with type 2 diabetes or impaired glucose tolerance [13]. Furthermore, supplementation with  $\text{H}_2$ -dissolved water normalized the oral glucose tolerance test in four out of six patients with impaired glucose tolerance. The reduction in the expression of biomarkers associated with systemic oxidative stress can be ascribed to the reductive property of  $\text{H}_2$  gas. The formation of 4-hydroxynonenal (HNE) through lipoprotein oxidation plays an etiologic role in atherosclerotic lesion progression [14,15]. Oxidized LDL is taken up by macrophages through scavenger

receptors, to form foam cells. Foam cells secrete growth factors that induce SMC migration from the media into the neointima. We demonstrate that the ingestion of  $\text{H}_2$ -dissolved water *ad libitum* for 6 months prevents the development of atherosclerosis in apolipoprotein E-knockout mice, which represent a model of spontaneously developing atherosclerosis [16]. This anti-atherogenic effect of  $\text{H}_2$ -dissolved water is associated with a reduction of HNE immunoreactivity in the aorta. These results suggest that persistent intake of  $\text{H}_2$  has the potential to reduce oxidative stress and may prevent cardiovascular disease.

### 3. Unexpected benefit of flatulence caused by $\alpha$ -glucosidase inhibitors

Is there any other way to supply  $\text{H}_2$  to the body?  $\text{H}_2$  is not produced endogenously in mammalian cells, since the hydrogenase activity responsible for the formation of  $\text{H}_2$  gas may not be present [17]. Instead, spontaneous production of  $\text{H}_2$  gas in the human body occurs via the fermentation of undigested carbohydrates by the resident enterobacterial flora.  $\text{H}_2$  is transferred to the portal circulation and excreted through the breath in significant amounts [18]. Flatulence is regarded as the major side-effect of treatment with  $\alpha$ -glucosidase inhibitors [19]. Therefore, we examined whether the administration of  $\alpha$ -glucosidase inhibitors increases the levels of  $\text{H}_2$  production in the gastrointestinal tract. Eleven healthy volunteers (10 males and 1 female) were administered acarbose at a dosage of 300 mg/day (100 mg three times a day) for 4 days under free-feeding conditions (Table 1). On Day 4 of the experiment, the levels of exhaled  $\text{H}_2$  and methane ( $\text{CH}_4$ ) were measured using the Breath Gas Analyzer Model TGA-2000 (TERAMECS, Kyoto, Japan). Acarbose treatment significantly increased the amount of exhaled  $\text{H}_2$  at every time-point examined ( $n = 11$ ,  $P < 0.05$ , paired  $t$ -test, as compared to before treatment with acarbose), whereas it had modest effects on  $\text{CH}_4$  production (Fig. 1). Acarbose treatment had no effect on  $\text{H}_2$  or  $\text{CH}_4$  production in 2/11 volunteers.

Kajiyama treated patients with type 2 diabetes or impaired glucose tolerance with 900 ml/day (300 ml three times a day)  $\text{H}_2$ -dissolved water. After drinking 300 ml of  $\text{H}_2$ -dissolved water, the exhaled  $\text{H}_2$  gas concentration reached a maximum of  $56 \pm 27.8$  ppm at 15 min, and returned to the baseline level at 150 min. This peak level of  $\text{H}_2$  gas reduced the levels of oxidative stress biomarkers and improved glucose metabolism in patients with type 2 diabetes or impaired glucose tolerance [13]. In the present study, we show that oral administration of acarbose at a dosage of 300 mg/day (100 mg given three times a day) can reach

**Table 1**

Eleven healthy volunteers (10 males and 1 female) were administered acarbose at a dosage of 300 mg/day (100 mg three times a day) for 4 days under free-feeding conditions. Exhaled gas was collected in an aluminium bag at the point of mid-expiration at the indicated time-points (i.e., morning, before lunch, 2 h after lunch, before retiring), both before and after acarbose treatment. The exhaled gas samples were injected into the Breath Gas Analyzer to measure the  $\text{H}_2$  and  $\text{CH}_4$  concentrations.

Sex	Hydrogen								Methane							
	Before				After				Before				After			
	Morning	Before lunch	After lunch	Before retiring	Morning	Before lunch	After lunch	Before retiring	Morning	Before lunch	After lunch	Before retiring	Morning	before lunch	After lunch	Before retiring
M	1	2	11	10	34	21	74	90	0	3	2	2	8	3	9	9
M	8	6	3	1	17	25	48	19	4	4	2	2	4	4	6	3
M	46	14	20	20	76	32	52	56	5	2	2	3	7	4	5	6
M	3	6	3	8	85	44	58	91	23	34	20	19	11	9	8	12
M	43	31	25	10	64	62	62	45	4	32	2	2	8	6	6	5
M	8	3	9	13	20	24	40	41	1	1	3	5	4	4	5	7
M	37	15	17	11	30	53	46	38	5	2	1	1	5	5	3	5
F	10	30	32	29	54	15	14	30	2	8	7	8	11	7	6	7
M	15	2	5	6	26	20	33	11	5	1	1	2	7	6	8	4
M	52	44	56	42	38	54	31	49	18	15	18	17	10	16	12	16
M	5	5	1	21	3	5	21	70	11	22	14	44	29	27	38	50

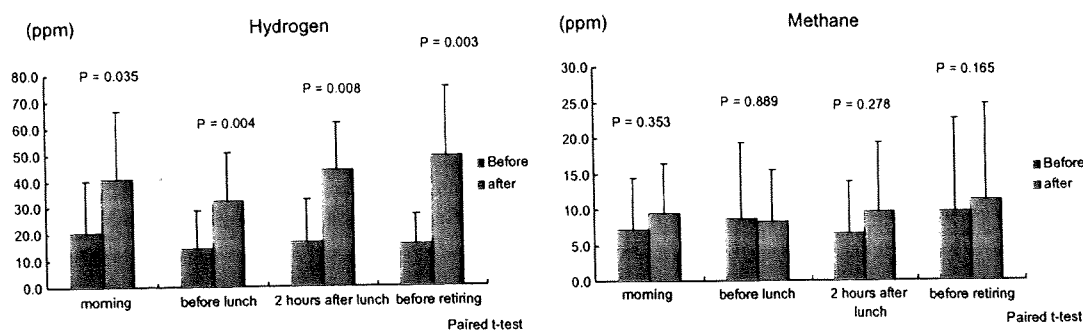


Fig. 1. Effects of acarbose on the levels of exhaled H<sub>2</sub> and CH<sub>4</sub>. The values shown in the bar graphs are means  $\pm$  S.D.

the same maximum levels of exhaled H<sub>2</sub> gas as compared to the consumption of 300 ml of H<sub>2</sub>-dissolved water. Moreover, acarbose maintained this peak level continuously. It is noteworthy that the breath concentration of H<sub>2</sub> on a fasting morning remains high in people who take acarbose. These observations clearly indicate that the amounts of H<sub>2</sub> gas generated by acarbose in our current experiments are sufficient to reduce systemic oxidative stress. Oral administration of acarbose may be superior to drinking H<sub>2</sub>-rich water in terms of maintenance of the appropriate H<sub>2</sub> gas levels in the body.

#### 4. Conclusion

Based on these observations and experimental results, we propose that  $\alpha$ -glucosidase inhibitors reduce the risk of cardiovascular disease in patients with impaired glucose tolerance or type 2 diabetes, and that these benefits can be attributed at least in part to the abilities of these drugs to neutralise oxidative stress by increasing the production of H<sub>2</sub> in the gastrointestinal tract. To investigate the relationship between the cardiovascular benefits of  $\alpha$ -glucosidase inhibitors and H<sub>2</sub> gas production by the gut microbiota, we should examine whether the cardiovascular benefits afforded by these drugs are diminished by scavenging H<sub>2</sub> gas in the gastrointestinal tract before absorption into the blood stream.

#### Conflict of interest statement

None declared.

#### Acknowledgement

This work was supported by a PRESTO (Metabolism and Cellular Function) Grant from the Japan Science and Technology Agency to M. Sano.

#### References

- [1] Coutinho, M., Gerstein, H.C., Wang, Y. and Yusuf, S. (1999) The relationship between glucose and incident cardiovascular events. A meta-regression analysis of published data from 20 studies of 95,783 individuals followed for 12.4 years. *Diabetes Care* 22, 233–240.
- [2] Barrett-Connor, E. and Ferrara, A. (1998) Isolated postchallenge hyperglycemia and the risk of fatal cardiovascular disease in older women and men. The rancho bernardo study. *Diabetes Care* 21, 1236–1239.
- [3] Chiasson, J.L., Josse, R.G., Gomis, R., Hanefeld, M., Karasik, A. and Laakso, M. (2003) Acarbose treatment and the risk of cardiovascular disease and hypertension in patients with impaired glucose tolerance: the STOP-NIDDM trial. *JAMA* 290, 486–494.
- [4] Hanefeld, M., Cagatay, M., Petrowitsch, T., Neuser, D., Petzinna, D. and Rupp, M. (2004) Acarbose reduces the risk for myocardial infarction in type 2 diabetic patients: meta-analysis of seven long-term studies. *Eur. Heart J.* 25, 10–16.
- [5] (1998) Intensive blood-glucose control with sulphonylureas or insulin compared with conventional treatment and risk of complications in patients with type 2 diabetes (UKPDS 33). UK Prospective Diabetes Study (UKPDS) Group. *Lancet* 352, 837–853.
- [6] Frantz, S., Calvillo, L., Tillmanns, J., Elbing, I., Dienesch, C., Bischoff, H., Ertl, G. and Bauersachs, J. (2005) Repetitive postprandial hyperglycemia increases cardiac ischemia/reperfusion injury: prevention by the  $\alpha$ -glucosidase inhibitor acarbose. *FASEB J.* 19, 591–593.
- [7] Madamanchi, N.R., Hakim, Z.S. and Runge, M.S. (2005) Oxidative stress in atherogenesis and arterial thrombosis: the disconnect between cellular studies and clinical outcomes. *J. Thromb. Haemost.* 3, 254–267.
- [8] Touyz, R.M. (2004) Reactive oxygen species, vascular oxidative stress, and redox signaling in hypertension: what is the clinical significance? *Hypertension* 44, 248–252.
- [9] Wilcox, C.S. (2003) Redox regulation of the afferent arteriole and tubuloglomerular feedback. *Acta Physiol. Scand.* 179, 217–223.
- [10] Steinhilber, S.R. (2008) Why have antioxidants failed in clinical trials? *Am. J. Cardiol.* 101, 14D–19D.
- [11] Ohsawa, I. et al. (2007) Hydrogen acts as a therapeutic antioxidant by selectively reducing cytotoxic oxygen radicals. *Nat. Med.* 13, 688–694.
- [12] Hayashida, K. et al. (2008) Inhalation of hydrogen gas reduces infarct size in the rat model of myocardial ischemia-reperfusion injury. *Biochem. Biophys. Res. Commun.* 373, 30–35.
- [13] Kajiyama, S. et al. (2008) Supplementation of hydrogen-rich water improves lipid and glucose metabolism in patients with type 2 diabetes or impaired glucose tolerance. *Nutr. Res.* 28, 137–143.
- [14] Lusis, A.J. (2000) Atherosclerosis. *Nature* 407, 233–241.
- [15] Berliner, J.A. and Watson, A.D. (2005) A role for oxidized phospholipids in atherosclerosis. *N Engl. J. Med.* 353, 9–11.
- [16] Ohsawa, I., Nishimaki, K., Yamagata, K., Ishikawa, M. and Ohta, S. (2008) Consumption of hydrogen water prevents atherosclerosis in apolipoprotein E knockout mice. *Biochem. Biophys. Res. Commun.* 377, 1195–1198.
- [17] Adams, M.W., Mortenson, L.E. and Chen, J.S. (1980) Hydrogenase. *Biochim. Biophys. Acta* 594, 105–176.
- [18] Levitt, M.D. (1969) Production and excretion of hydrogen gas in man. *N Engl. J. Med.* 281, 122–127.
- [19] Ladas, S.D., Frydas, A., Papadopoulos, A. and Raptis, S.A. (1992) Effects of  $\alpha$ -glucosidase inhibitors on mouth to caecum transit time in humans. *Gut* 33, 1246–1248.

## Molecular hydrogen alleviates nephrotoxicity induced by an anti-cancer drug cisplatin without compromising anti-tumor activity in mice

Naomi Nakashima-Kamimura · Takashi Mori · Ikuroh Ohsawa · Sadamitsu Asoh · Shigeo Ohta

Received: 24 September 2008 / Accepted: 30 December 2008 / Published online: 16 January 2009  
© Springer-Verlag 2009

### Abstract

**Purpose** Cisplatin is a widely used anti-cancer drug in the treatment of a wide range of tumors; however, its application is limited by nephrotoxicity, which is affected by oxidative stress. We have reported that molecular hydrogen (H<sub>2</sub>) acts as an efficient antioxidant (Ohsawa et al. in *Nat Med* 13:688–694, 2007). Here we show that hydrogen efficiently mitigates the side effects of cisplatin by reducing oxidative stress.

**Methods** Mice were administered cisplatin followed by inhaling hydrogen gas (1% H<sub>2</sub> in air). Furthermore, instead of inhaling hydrogen gas, we examined whether drinking water containing hydrogen (hydrogen water; 0.8 mM H<sub>2</sub> in water) is applicable by examining oxidative stress, mortality, and body-weight loss. Nephrotoxicity was assessed by morphological changes, serum creatinine and blood urea nitrogen (BUN) levels.

**Results** Inhalation of hydrogen gas improved mortality and body-weight loss caused by cisplatin, and alleviated nephrotoxicity. Hydrogen was detected in blood when hydrogen water was placed in the stomach of a rat. Consuming hydrogen water ad libitum also reduced oxidative stress, mortality, and body-weight loss induced by cisplatin in mice. Hydrogen water improved metamorphosis accompanying decreased apoptosis in the kidney, and nephrotoxicity as assessed by serum creatinine and BUN levels. Despite its protective effects against cisplatin-induced toxicity, hydrogen did not impair anti-tumor activity of cisplatin against cancer cell lines in vitro and tumor-bearing mice in vivo.

**Conclusion** Hydrogen has potential for improving the quality of life of patients during chemotherapy by efficiently mitigating the side effects of cisplatin.

**Keywords** Antioxidant · Cisplatin · Dihydrogen · Oxidative stress · Side effect

N. Nakashima-Kamimura · I. Ohsawa · S. Asoh · S. Ohta (✉)  
Department of Biochemistry and Cell Biology,  
Institute of Development and Aging Sciences,  
Nippon Medical School, Kawasaki,  
Kanagawa 211-8533, Japan  
e-mail: ohta@nms.ac.jp

I. Ohsawa  
The Center of Molecular Hydrogen Medicine,  
Institute of Development and Aging Sciences,  
Nippon Medical School, Kawasaki,  
Kanagawa 211-8533, Japan

T. Mori  
Institute of Medical Science,  
Saitama Medical Center/University,  
Kawagoe, Saitama 350-8550, Japan

### Introduction

The development of chemotherapeutic drugs exhibiting weak side effects is desired; at the same time, overcoming side effects is essential for the clinical use of anti-cancer drugs. Cisplatin (*cis*-diamminedichloroplatinum II) is currently one of the most effective chemotherapeutic agents in the treatment of a variety of tumors, including those of the head, neck, testis, ovary and breast [1]. Higher doses of cisplatin are more efficacious; however, high-dose therapy is limited by nephrotoxic side effects [2]. Cisplatin causes the accumulation of reactive oxygen species (ROS), such as superoxide anions and hydroxyl radicals, by suppressing antioxidant activity through decreasing the reduced form of